NOAA Technical Memorandum
NWS TDL 78

OBJECTIVE ASSESSMENT OF 1984-85 VAS PRODUCTS AS INDICES OF THUNDERSTORM AND SEVERE LOCAL STORM POTENTIAL

Techniques Development Laboratory
Silver Spring, MD
March 1988

U.S. DEPARTMENT OF COMMERCE / National Oceanic and Atmospheric Administration / National Weather Service

NOAA TECHNICAL MEMORANDUMS

National Weather Service, Techniques Development Laboratory Series

The primary purpose of the Techniques Development Laboratory of the Office of Systems Development is to translate increases of basic knowledge in meteorology and allied disciplines into improved operating techniques and procedures. To achieve this goal, the Laboratory conducts applied research and development aimed at the improvement of diagnostic and prognostic methods for producing weather information. The Laboratory performs studies both for the general improvement of prediction methodology used in the National Meteorological Service and for the more effective utilization of weather forecasts by the ultimate user.

NOAA Technical Memorandums in the National Weather Service Techniques Development Laboratory series facilitate rapid distribution of material that may be preliminary in nature and which may be published formally elsewhere at a later date. Publications 1 through 5 are in the former series Weather Bureau Technical Notes (TN), Techniques Development Laboratory (TDL) Reports; publications 6 through 36 are in the former series ESSA Technical Memorandums, Weather Bureau Technical Memorandum, (WBTM). Beginning with TDL 37, publications are now part of the series NOAA Technical Memorandums, National Weather Service (NWS).

Publications listed below are available from the National Technical Information Service, U.S. Department of Commerce, Sills Bldg., 5285 Port Royal Road, Springfield, VA 22161. Prices on request. Order by accession number (given in parentheses).

ESSA Technical Memorandums

WBTM TDL 17 Second Interim Report on Sea and Swell Forecasting. N. A. Pore and W. S. Richardson, January 1969, 7 pp. plus 10 figures. (PB-182-273)

WBTM TDL 18 Conditional Probabilities of Precipitation Amounts in the Conterminous United States. Donald L. Jorgensen, William H. Klein, and Charles F. Roberts, March 1969, 89 pp. (PB-183-144)

WBTM TDL 19 An Operationally Oriented Small-Scale 500-Millibar Height Analysis Program. Harry R. Glahn and George W. Hollenbaugh, March 1969, 17 pp. (PB-184-111)

WBTM TDL 20 A Comparison of Two Methods of Reducing Truncation Error. Robert J. Bermowitz, May 1969, 7 pp. (PB-184-741)

WBTM TDL 21 Automatic Decoding of Hourly Weather Reports. George W. Hollenbaugh, Harry R. Glahn, and Dale A. Lowry, July 1969, 27 pp. (PB-185-806)

WBTM TDL 22 An Operationally Oriented Objective Analysis Program. Harry R. Glahn, George W. Hollenbaugh, and Dale A. Lowry, July 1969, 20 pp. (PB-186-129)

WBTM TDL 23 An Operational Subsynoptic Advection Model. Harry R. Glahn, Dale A. Lowry, and George W. Hollenbaugh, July 1969, 26 pp. (PB-186-389)

WBTM TDL 24 A Lake Erie Storm Surge Forecasting Technique. William S. Richardson and N. Arthur Pore, August 1969, 23 pp. (PB-185-778)

WBTM TDL 25 Charts Giving Station Precipitation in the Plateau States From 850- and 500-Millibar Lows During Winter. August F. Korte, Donald L. Jorgensen, and William H. Klein, September 1969, 9 pp. plus appendixes A and B. (PB-187-476)

WBTM TDL 26 Computer Forecasts of Maximum and Minimum Surface Temperatures. William H. Klein, Frank Lewis, and George P. Casely, October 1969, 27 pp. plus appendix. (PB-189-105)

WBTM TDL 27 An Operational Method for Objectively Forecasting Probability of Precipitation. Harry R. Glahn and Dale A. Lowry, October 1969, 24 pp. (PB-188-660)

WBTM TDL 28 Techniques for Forecasting Low Water Occurrence at Baltimore and Norfolk. James M. McClelland, March 1970, 34 pp. (PB-191-744)

WBTM TDL 29 A Method for Predicting Surface Winds. Harry R. Glahn, March 1970, 18 pp. (PB-191-745)

WBTM TDL 30 Summary of Selected Reference Material on the Oceanographic Phenomena of Tides, Storm Surges, Waves, and Breakers. N. Arthur Pore, May 1970, 103 pp. (PB-193-449)

WBTM TDL 31 Persistence of Precipitation at 108 Cities in the Conterminous United States. Donald L. Jorgensen and William H. Klein, May 1970, 84 pp. (PB-193-599)

WBTM TDL 32 Computer-Produced Worded Forecasts. Harry R. Glahn, June 1970, 8 pp. (PB-194-262)

WBTM TDL 33 Calculation of Precipitable Water. L. P. Harrison, June 1970, 61 pp. (PB-193-600)

WBTM TDL 34 An Objective Method for Forecasting Winds Over Lake Erie and Lake Ontario. Celso S. Barrientos. August 1970, 20 pp. (PB-194-586)

WBTM TDL 35 Probabilistic Prediction in Meteorology; a Bibliography. Allan H. Murphy and Roger A. Allen, June 1970, 60 pp. (PB-194-415)

WBTM TDL 36 Current High Altitude Observations--Investigation and Possible Improvement. M. A. Alaka and R. C. Elvander, July 1970, 24 pp. (COM-71-00003)

NWS TDL 37 Prediction of Surface Dew Point Temperatures. R. C. Elvander, February 1971, 40 pp. (COM-71-00253)

NWS TDL 38 Objectively Computed Surface Diagnostic Fields. Robert J. Bermowitz, February 1971, 23 pp. (COM-71-0301)

NWS TDL 39 Computer Prediction of Precipitation Probability for 108 Cities in the United States. William H. Klein, February 1971, 32 pp. (COM-71-00249)

NWS TDL 40 Wave Climatology for the Great Lakes. N. A. Pore, J. M. McClelland, C. S. Barrientos, and W. E. Kennedy, February 1971, 61 pp. (COM-71-00368)

NWS TDL 41 Twice-Daily Mean Heights in the Troposphere Over North America and Vicinity. August F. Korte, June 1971, 31 pp. (COM-71-0286)

NWS TDL 42 Some Experiments With a Fine-Mesh 500-Millibar Barotropic Model. Robert J. Bermowitz, August 1971, 20 pp. (COM-71-00958)

(Continued on inside back cover)

NOAA Technical Memorandum
NWS TDL 78

OBJECTIVE ASSESSMENT OF 1984-85 VAS PRODUCTS AS INDICES OF THUNDERSTORM AND SEVERE LOCAL STORM POTENTIAL

David H. Kitzmiller and Wayne E. McGovern

Techniques Development Laboratory
Silver Spring, MD
March 1988

UNITED STATES
DEPARTMENT OF COMMERCE
C. William Verity, Jr.
Secretary

National Oceanic and
Atmospheric Administration
Melvin N.A. Peterson
Acting Under Secretary

National Weather Service
Richard E. Hallgren
Assistant Administrator

Table of Contents

OBJECTIVE ASSESSMENT OF 1984-85 VAS PRODUCTS AS INDICES OF THUNDERSTORM AND SEVERE LOCAL STORM POTENTIAL

David H. Kitzmiller and Wayne E. McGovern

ABSTRACT

Objective experiments have been carried out to determine which VAS-derived moisture and stability indices contain the greatest amount of predictive information with respect to thunderstorm and severe local storm events. In these experiments, stability and moisture parameters derived from 1700 GMT VAS retrievals were compared and correlated to storm observations during the subsequent 2000-0000 GMT period. The amount of predictive information in these indices was also compared to that possessed by indices derived from VAS retrievals taken earlier in the day, and from concurrently-available radiosondes and numerical model forecasts. The correlation in the form of the computed information ratio (I_c) was used as a measure of predictive power in these experiments.

It was found that precipitable water and modified versions of the classic K index which included the latest surface data have the highest values of I_c for general thunderstorm occurrence. The 50-kPa gradient wind speed (derived from VAS geopotential heights) and the temperature lapse rate in the 70-50 kPa layer were the best predictors for discriminating severe local storm cases from general thunderstorm cases. The 3-h and 6-h changes in stability and moisture indices were poorly correlated to severe storm occurrence. Of all the variables examined, only the change in surface blackbody temperature appeared to be even moderately correlated to severe storms.

It was also found that updating of stability measureents leads to modest increases in predictive information. The retrievals appear to possess slightly more information with respect to thunderstorm occurrence than do their own first guess profiles, which are derived from a forecast of the LFM. In addition, the VAS-derived stability indices at 1700 GMT appear to possess more information than the same indices when derived from 1200 GMT raob measurements; however, indices derived from LFM forecasts valid near the observation period (2000-0000 GMT) have more information than the 1700 GMT VAS-based indices. Possible reasons for these findings, and their implications for future satellite operations and applied research, are discussed.

1. INTRODUCTION

Assessing the potential for thunderstorm and severe local storm occurrence several hours in advance requires some knowledge of the middle and upper troposphere's temperature, humidity, and winds. A large number of indices involving temperature, humidity, wind speed, and wind shear have been applied to convection forecasting (see, for example, Miller, 1972). For the past several decades, radiosondes have been the primary source of observations of these atmospheric variables. More recently, however, infrared radiation measurements from earth-orbiting satellites have been used to create temperature and moisture soundings that augment existing upper-air observations.

Since 1981, the National Environmental Satellite, Data and Information Service (NESDIS) has retrieved vertical profiles of temperature and moisture from measurements of the Visible and Infrared Spin Scan Radiometer (VISSR) Atmospheric Sounder (VAS). This sounding system (described by Smith et al., 1981) is carried aboard later versions of the Geostationary Operational Environmental Satellite (GOES). During the spring and early summer, a number of convective stability indices derived from VAS retrievals have been sent in near-real time to the National Severe Storms Forecast Center (NSSFC) for assessment by forecasters there. The results of this assessment have been summarized by Anthony and Wade (1983), Anthony and Leftwich (1984), Wade et al. (1985), and Shoeni and Mosher (1986).

To assist in this assessment, the National Weather Service's Techniques Development Laboratory (TDL) has investigated possible uses for VAS retrieval products in a number of its statistical forecasting systems. These guidance systems produce objective probability forecasts of thunderstorms and severe local storms over a number of time intervals (see Reap and Foster, 1979, and Charba, 1979 and 1984). The systems currently depend in part upon numerical forecasts of upper-air conditions.

In determining how VAS products might best be used in objective statistical guidance for forecasting convective phenomena, four major questions were considered:

(1) Which VAS-derived stability indices and combinations of indices are the most reliable predictors of thunderstorm or severe local storm occurrence?

(2) Do temporal changes of humidity and stability as measured by VAS consistently provide clues on the subsequent development of severe weather?

(3) To what extent can updating of stability measurements improve thunderstorm forecasts?

(4) Do the VAS retrievals contain more predictive information than concurrently-available radiosonde observations and operational numerical forecasts?

2. VAS DATA USED IN THIS STUDY

The VAS temperature and dew point profiles used in these experiments were prepared semi-operationally by personnel of the NESDIS Advanced Satellite

Products Project (ASPP) in Madison, Wisconsin. The retrievals were made during the months of March through July in 1984 and 1985 and were forwarded in near real time to NSSFC for experimental use by forecasters there. Satellite sounding operations were often precluded by the need for rapid-interval scanning to produce visible imagery for other forecasting applications, so that only about 76 days of retrievals are now available. The dataset contains soundings from VAS observations at 1100, 1300, 1400, and 1700 GMT. Retrievals were made over the United States east of the Rocky Mountains, though in most sets of soundings coverage gaps up to several hundred kilometers in diameter exist where dense cloud cover prevented retrievals from being made.

The profiles were retrieved via a physical regression algorithm in which temperature and moisture are determined simultaneously (Smith and Woolf, 1984). This algorithm differs substantially from earlier schemes, so profiles prepared prior to the 1984 season were excluded from this study. The new algorithm directly incorporates hourly surface observations of temperature and dew point, in order to increase the accuracy of the retrievals at lower levels.

While the VAS instrument was designed to monitor changes in atmospheric temperature and moisture over time, the unit aboard GOES 6 presently has mechanical problems that could impair its ability to detect such changes. Menzel and Schreiner (1985) have reported on the failure of the servo mechanism that initially maintained a constant VAS filter wheel temperature. Changes in the filter wheel temperature can cause unrealistic fluctuations in the retrieved mid-tropospheric temperatures over the course of the day. During the course of our experiments, however, we found very few cases in which the retrieved 50-kilopascal (50-kPa, or 500-mb) temperature changed radically during the 1400-1700 GMT period. Our results show no degradation in the predictive information content of stability indices between 1100 and 1700 GMT. While mechanical difficulties with the VAS instrument have some effect on the accuracy of the retrievals, existing errors do not appear to overwhelm the ability of VAS to detect changes in the atmospheric state.

3. VERIFICATION DATA

Surface reports of audible thunder cannot be relied upon to provide a complete summary of general thunderstorm occurrence, due to the sparse distribution of observing stations. We also currently lack a standardized archive of remotely-sensed lightning reports covering the entire United States. Therefore, we have followed the practice used by Reap and Foster (1979, hereafter referred to as RF) and by Charba (1984, referred to as CH84) of inferring the occurrence of thunderstorms from radar observations. As shown by RF, radar echoes of Video Integrator and Processor (VIP) level 3 or greater are strongly correlated to thunderstorm activity. The TDL archive of manually-digitized radar (MDR) data shows the maximum VIP level of all echoes within 80-km square grid blocks during each hour. We assume that a thunderstorm occurred if an echo of VIP level 3 or greater was observed within a grid block during the verification period.

Reports of tornadoes, surface hail of diameter $\geq$ 2 cm, and convective wind gusts $\geq$ 93 km h^{-1} or wind damage are routinely collected and edited at the NSSFC. These reports have been tabulated for each hour and for each block of the 80-km radar archive grid. A severe local storm was considered to have occurred if at least one of these convective phenomena was observed within a grid block during the verification period.

The primary emphasis of this study was determining the impact of VAS retrievals upon short-range (0-10 h) thunderstorm forecasts. Therefore, most of our statistical comparisons were made with retrievals prepared from 1700 GMT irradiance measurements, and weather observations during the subsequent period 2000-0000 GMT. This 3-h time lag reflects operational constraints, namely the minimum time required to ingest the satellite data, prepare and edit the retrievals, and prepare and disseminate a forecast with some lead time. The 2000-0000 GMT valid period corresponds to one of the periods now covered by operational 2-6 h thunderstorm and severe local storm forecasts (Charba, 1979, and CH84).

4. OBJECTIVE ASSESSMENT OF THE CONVECTION PREDICTORS' INFORMATION CONTENT

To judge the ability of the predictors to indicate storm potential, we used the computed information ratio (I_c) developed by Holloway and Woodbury (1955). The abbreviation I_c was adopted from Keller and Smith (1983), to avoid confusion with the common abbreviation for "infrared radiation". In a form similar to that shown below, the I_c was used by Lund and Wahl (1955) in experiments in statistical weather forecasting, and by Keller and Smith in a comparison of convective stability indices derived from rawindsondes and satellite measurements. In our particular application, the I_c serves as a flexible measure of the correlation between a predictor and the observed relative frequency of storm events. To compute I_c, the continuous predictor values (K index, for example) are stratified into a number of classes, and the number of cases with and without storm events is tabulated for each class. If there are k classes, and if the predictand is divided into two categories (storm/no storm), the information ratio may be defined:

$$I_c = \frac{N \ln(N) - M \ln(M) - P \ln(P) + \sum_{i=1}^{k} S_i \ln(S_i) + O_i \ln(O_i) - E_i \ln(E_i)}{N \ln(N) - M \ln(M) - P \ln(P)}$$

where i is the index of the predictor class,
E_i is the number of cases in class i,
S_i is the number of storm cases in class i,
O_i is the number of nonstorm cases in class i,
N is the total number of cases,
M is the total number of storm cases, and
P is the total number of nonstorm cases.

The I_c ranges in value from zero to one. If the predictor has perfect information (if each class features only storm or nonstorm events), then the summation term in the fraction above vanishes and I_c is equal to unity. If the predictor has no information (the event relative frequency is the same in all classes), then I_c vanishes. Since the I_c represents a measure of predictive information, we sometimes refer to I_c as a measure of "information content."

In practice, the sample was divided into enough categories to provide a good representation of the storm frequency's dependence upon the predictor values. At the same time it was necessary to keep enough cases in each category to be

sure that a representative sample was obtained. In comparing values of I_c for different predictors, or comparing values of I_c for the same predictor when derived from different observational data, we insured that the sample of cases was precisely matched; that is, if the value for any one predictor was missing for a given location at a given time, the case was eliminated from consideration in computing I_c for all other predictors as well.

A prime reason for our use of the I_c as a correlation measure is that the I_c is not seriously influenced by a nonlinear relationship between the predictor and predictand, as is the linear correlation coefficient. As noted by Charba (1979) and by RF, stability indices often have a markedly nonlinear relationship to storm relative frequency. In such cases, the linear correlation coefficient of such indices does not reveal their true relative predictive potential. The I_c is based solely upon the observed storm frequency within various classes of events defined by the predictor magnitude. Thus I_c does not depend upon the nature of the relationship (e.g. linear, logarithmic) between the observed storm frequency and the predictor itself.

The biserial correlation coefficient (Panofsky and Brier, 1968) may also be used to describe the strength of the correlation between a stability index and the likelihood of convective storms (see Stone, 1985). This coefficient depends upon the difference between the mean predictor value for all storm cases and the mean value for all nonstorm cases. If the relationship between the stability index and event relative frequency is not monotonic, however, the biserial coefficient will again not accurately reveal the relative predictive potential of the index. For example, the observed storm frequency might peak at both large and small index values. In this case, the mean index values for storm and nonstorm cases will approach each other, and the biserial correlation will be small even though there is a strong predictor/predictand relationship.

In practice, the nonlinearity between the predictor and predictand may be dealt with by performing a mathematical transformation of the original stability indices to ensure a linear relationship to the predictand relative frequency. The form of the transformation must be determined empirically from the available data. The transformed predictor linearly corresponds to the observed event relative frequency for any given value of the original index. Both RF and CH84 used this technique in deriving convective probability predictors. An advantage in using the I_c is that it provides a direct estimate of the predictive potential of the stability indices, even before the time-consuming linearization process is undertaken.

To facilitate our comparison of the predictors to subsequent storm observations, we calculated all of the predictors at the nominal retrieval locations and interpolated their values to the central points of the MDR archive grid using a two-pass Barnes (1973) analysis scheme. While the average spatial separation between retrievals is approximately 100 km, the density of soundings varies greatly due to cloud gaps. Because the analyzed fields may contain erroneous values in the observation gaps, all grid blocks that were more than two grid increments away from the nearest retrieval were eliminated from consideration.

The region of interest in this study includes 542 grid blocks over the central United States east of the Rocky Mountains and west of the Appalachian Mountains. Grid blocks north of the 45th parallel of latitude and over the Gulf of Mexico were excluded.

For the testing of predictors derived from 1700 GMT VAS data, over 30,000 cases were available (76 days times 542 grid blocks minus blocks excluded due to cloud gaps or missing radar reports). In computing I_c, we divided the entire sample into predictor categories in such a way that nearly the same number of cases fell into each category. This was done to insure that our comparison among I_c values from the different predictors wasn't affected by the choice of class intervals.

5. STABILITY INDICES TESTED AS GENERAL THUNDERSTORM PREDICTORS

Earlier work (RF; CH84; Kitzmiller, 1985) has shown that substantial information on general thunderstorm potential can be obtained from a single stability index that depends upon the temperature and moisture stratification in the lower troposphere. In developing their objective guidance system for 12-36 h thunderstorm forecasts, RF found that the classic K index and climatic thunderstorm frequency formed the combination of predictors best-correlated to storm events. In CH84, it was shown that a predictor combining the K index and observed surface moisture divergence was the one most strongly correlated to thunderstorms over the 2-6 h period. In both types of forecasts, additional predictors such as low-level moisture divergence tended to add only a relatively small amount of information to that provided by the K index. Accordingly, we began our study by comparing the computed information ratios of several basic indices that describe the stability and vertically-averaged humidity.

The K index is a linear combination of temperature and dew point values at various levels:

$$K = (T_{85} - T_{50}) + DP_{85} - (T_{70} - DP_{70})$$

(George, 1954) where T is temperature in degrees C, DP is dew point in degrees C, and the subscripts represent the pressure level in kilopascals. The K index reflects the temperature lapse rate and the humidity between the surface and the 70 kPa level. As shown by RF and by CH84, it is a powerful predictor of thunderstorm potential. We have tested two other versions of the K index, a modified K index (MK) introduced by CH84, and the surface K index (SK). These are defined:

$$MK = 0.5(T_{85} + T_{sfc}) - T_{50} + 0.5(DP_{85} + DP_{sfc}) - (T_{70} - DP_{70})$$

$$SK = (T_{sfc} - T_{500}) + DP_{sfc} - (T_{70} - DP_{70})$$

Here, surface observations of temperature and dew point (subscripted "sfc") have been incorporated. These surface terms are obtained from the standard hourly measurements and generally have high absolute accuracy.

The lifted index, or LI (Galway, 1956), is defined as the difference between the temperature at the 50-kPa level and the temperature of a parcel lifted to that level from the surface. This parcel is assumed to rise adiabatically to its lifting condensation level, then pseudo-adiabatically. In a conditionally unstable atmosphere, the parcel will be warmer than the environment at 50 kPa, and the index is negative. The Showalter index (Showalter, 1953) is computed in the same manner, except that the rising parcel is lifted from the 85-kPa level.

Both the Showalter and lifted indices make use of temperature data at only two levels. Recently, a number of indices have been introduced that make use of the data at all available levels. One such index is the change in buoyant energy (PBE) realized by a parcel as it rises from its level of free convection to its equilibrium level. We have defined this index in a manner similar to that given by Stone (1985):

$$PBE = -R \int_{LFC}^{EQL} (T' - T)\, d\ln(p)$$

where R is the gas constant, T' the rising parcel's temperature, T the environment's temperature, and p the pressure. The terms LFC and EQL stand for pressure at the level of free convection and the equilibrium level.

Three additional predictors of thunderstorm occurrence were obtained from an entraining jet model of cumulus clouds. This model is similar to that developed by Simpson and Wiggert (1969), and has been tested in thunderstorm forecasting applications (Sanders and Garrett, 1975; Crum and Cahir, 1983; Kitzmiller, 1985). The model requires as input only the temperature and moisture stratification from the VAS retrieval; other cloud properties such as radius and initial updraft speed are specified. The model-derived cloud depth, maximum updraft speed, and rainfall were selected for testing as potential predictors. Each of these terms had been found in earlier studies to be strongly-correlated to thunderstorm likelihood.

6. RESULTS OF THE COMPARISON AMONG THUNDERSTORM PREDICTORS

To compute I_c for the thunderstorm predictors, we divided the data sample into 14 predictor classes, with approximately 2200 cases falling into each class. Thunderstorm frequency within the sample was about 12%. A graphical display of the ten highest I_c values and their associated predictors appears in Fig. 1.

While the SK index has the highest information ratio, the relative frequency distributions for all predictors with I_c greater than 0.24 appear very similar. Note that the precipitable water (PW) has a high information ratio, even though it contains no stability information per se. Precipitable water is probably so strongly correlated to convection potential because total water vapor is dependent upon large-scale moisture convergence. Furthermore, there is a strong relationship between the climatic mean of PW and the climatic thunderstorm relative frequency.

Note that the incorporation of surface observations of temperature and dew point seems to increase stability information. The modified versions of the K index (MK and SK) have larger I_c values than does the K index itself; similarly LI has a larger I_c than the Showalter index.

When I_c is computed from a limited data sample, the possibility exists that some information appears by chance alone. The value of I_c will tend toward zero in an infinite data sample if there is no relationship between predictor and predictand. If the data sample is limited, as it is in these experiments, there is usually some random variation in the event relative frequency from one category to the next. These variations can cause appreciable values of I_c. As stated by Lund and Wahl (1955), it is possible to estimate the largest value

of I_c that might be found for a quantity that in fact has no predictive information.

If there is, in fact, no relationship between the predictor and the predictand relative frequency, then the numerator term in the expression for I_c is distributed approximately as one-half "chi-squared" with (k-1) degrees of freedom, where k is the number of predictor categories. The denominator depends only upon the number of storm and nonstorm cases in the data sample. Thus the maximum expected value of the numerator at various confidence levels may be obtained from tables of chi-squared values, and these numerator values used in combination with the known denominator to estimate the maximum expected value of I_c due strictly to chance. For the overall thunderstorm frequency observed within the case sample used in this experiment, there is only a 5% chance that a predictor with no information on thunderstorm occurrence would yield an I_c greater than about 0.001. Thus there is very little likelihood that the predictive information of any of the indices mentioned previously is due strictly to chance.

It should be noted that this "random" I_c should not be interpreted as a confidence limit on the estimate of I_c itself. Holloway and Woodbury (1956) state that estimates of I_c have an F-distribution whose precise form is unknown. Due to sample irregularities and observational errors, the true confidence limit on I_c must be larger than the random I_c.

The observed thunderstorm relative frequency as a function of the SK index appears in Fig. 2. In this and all other similar figures, the abscissa values are the breakpoint values between categories. Therefore the height of the leftmost box represents the thunderstorm relative frequency for all cases in which the SK index was less than 17°C. The height of the box immediately to its right represents the frequency for all cases in which SK was greater than or equal to 17°C but less than 22°C, and so on. Over a large range of lower SK values, the storm relative frequency is nearly zero; the index is also capable of delineating regions in which the thunderstorm frequency is greater than 50%, or more than four times the overall frequency within the sample. In this and all other relative frequency figures, we usually show unevenly-spaced predictor category dividers. This spacing reflects the distribution of the predictor values themselves; the different categories all contain samples of nearly equal size.

To demonstrate the manner in which the I_c reflects predictive potential, we show the relative frequency distribution for the Total Totals index in Fig. 3. We found that this index had a much smaller value of I_c than did the SK index. Note that the distribution is relatively "flat" when compared to the distribution for the SK index, and that the largest frequency value is only approximately 30%. The Total Totals index thus appears to have limited capability for delineating regions of small or very large thunderstorm potential.

Thunderstorm relative frequency distributions for other selected predictors appear in Figs. 4-6.

7. INFORMATION CONTENT OF VARIOUS PREDICTORS IN COMBINATION WITH THE SK INDEX

While considerable predictive information is contained in the SK index, other factors that encourage or inhibit thunderstorm development should be considered

in forecasting. To examine the influence that other factors have upon thunderstorm potential, we constructed a set of "interactive" predictor tables in which thunderstorm relative frequency appears as a function of the SK index and another variable simultaneously. This technique was earlier used by CH84 and by Keller and Smith (1983).

We computed I_c values for these tables from the formula given earlier; eight classes were established for each predictor, so the total number of classes is 64. The predictor class breakpoints were selected so that at least 200 cases fell into the highest-probability classes. In selecting predictors for these tables, we concentrated upon those indices which are known to be correlated to thunderstorms but which are probably not strongly correlated to SK. An explanation of some of these indices follows.

The negative buoyant energy (NBE) is the kinetic energy required to raise a parcel from the surface to its level of free convection. As pointed out by Purdom (1985) and Stone (1985), this quantity is large in a column that has a strong capping inversion. The NBE is computed from the formula given earlier for PBE, except that the limits of integration are now the surface pressure and pressure at the LFC. The 50-kPa wind speed is the gradient wind speed computed from the VAS-derived 50-kPa geopotential height field. The derived gradient winds were included in the retrieval dataset provided to us by NESDIS. The 70-50 kPa lapse rate (TLPS) is the average temperature lapse rate within that layer; the layer thickness was estimated from the 70- and 50-kPa temperatures, using the hypsometric formula.

Certain predictors were derived from objective analyses of hourly surface reports. The 1700 GMT VAS retrievals incorporate 1600 GMT surface observations, so to maintain consistency we employed 1600 GMT observations in making the surface analyses. Analyses of temperature, dew point, terrain pressure, and u- and v-wind were prepared with the Cressman-type scheme used by CH84. Since these analyses are based upon all available surface observations, they are not affected by the cloud gaps that appear in the VAS data.

One surface-data index sometimes used in convection forecasting, the modified lifting condensation level (MLCL), is defined:

$$\begin{aligned} MLCL &= DP_{sfc} - (T_{sfc} - DP_{sfc}) \\ &= 2DP_{sfc} - T_{sfc} \end{aligned}$$

after Livingston and Darkow (1979). This index is related to the altitude of the lifting condensation level through the dew point depression term; it is highest in regions of high dew point and high relative humidity. Moisture divergence and equivalent potential temperature advection (θ_e) were considered since they were found by CH84 to be correlated to thunderstorm activity.

Both RF and CH84 have incorporated climatic event relative frequency into convection predictors. Our climatic frequency values have been estimated from all available radar reports during the period 1974-1983. This particular climatic frequency is computed for each grid block for each month; the daily climatic frequency is obtained by assuming the monthly frequency is valid on the 15th of the month, and interpolating to the given day of the month. The relative frequency values themselves are for a 24-h period.

The values of I_c for the predictor combinations appear in Fig. 7. Additional predictors all added approximately the same amount of information; nevertheless the combinations of SK with NBE, MLCL, and surface moisture divergence possess the greatest information. Other predictors such as LI and PW, which are correlated fairly strongly to the SK index, seem to add the least information. Observed thunderstorm relative frequency as a function of SK and NBE appears in Fig. 8. While the largest relative frequency, 52%, is barely higher than the largest value in the SK histogram, we see that many classes have very low frequency values. Thus it appears that NBE adds information by delineating areas of high SK index in which convection is still unlikely because of low-level capping.

Using multiple linear regression, we obtained the following least-squares approximation to the relationship between SK, NBE, and the observed thunderstorm frequency:

$$P = -3200 + [120SK] - [NBE/2]$$

where P is probability in per cent, SK is in degrees C, and NBE is in J kg^{-1}.

8. COMPARISON AMONG PREDICTORS OF SEVERE LOCAL STORM POTENTIAL

Our second series of experiments was designed to demonstrate which observeable quantities are the best predictors of conditional severe local storm probability, that is, the probability of severe local storms given that any thunderstorm activity occurs. While we initially investigated the prediction of absolute severe storm probability, the results were disappointing. It became apparent that two or even more predictors considered together could not delineate regions with a severe storm potential much greater than 6%, which was the percentage of all thunderstorm cases with severe local storms in the data sample. Furthermore, the best thunderstorm predictors turned out to be the best severe storm predictors. Thus, our selection of predictors had little skill in differentiating the severe storm environment from the general thunderstorm environment. Had the data sample been larger, the results might well have been better.

We therefore approached the severe storm problem using the method followed by RF, namely predicting the probability of severe weather within areas that experience convective activity. In constructing the relative frequency tables shown later, we considered only those cases in which radar echoes of VIP level 3 or greater were observed during the verification period. Those cases which also had severe weather reports (damaging winds, large hail or tornadoes) were considered to be the "storm" events within the sample. Predictors that are strongly correlated to such severe events in the sample of thunderstorm cases are the ones best able to differentiate between the general convective and severe local storm environments.

Within well-organized synoptic-scale systems, severe storms generally occur in regions of strong mid-tropospheric winds and low-level warm advection as indicated by wind vectors turning clockwise with height (see Miller, 1972). Severe storm areas are also characterized by upward motion and low sea-level pressure, as shown by RF. We examined a number of predictors that reflect these conditions. It has also been noted that environments in which mixing ratio decreases rapidly with height are prone to severe storms (Mostek et al., 1986). We tested the 70-50 kPa mean relative humidity as a predictor. Doswell

et al. (1985) have reported that the geometric temperature lapse rate within the 70-50 kPa layer tends toward larger values in severe weather situations, and this lapse rate was examined. Finally, a number of the stability indices found to be well-correlated to general convection were also tested.

Approximately 4300 thunderstorm cases were available for this experiment, of which 277, or 6%, had associated severe weather reports. (Those few events in which severe reports came from grid blocks having no VIP-3 echoes were included as severe cases.) As before, the predictors were derived from 1700 GMT VAS retrievals, and the verification period for severe storm observations was 2000--0000 GMT. To compute I_c, we divided the predictor sample into seven categories, with 610 cases in each.

The values of I_c with respect to conditional severe storm occurrence for some of these predictors are shown in Fig. 9. The standard stability indices (such as the SK index and LI) appear to be relatively poor predictors of severe storm activity within active convection areas. The Total Totals index (not shown) also had a very low I_c. The variables involving vertical wind shear (not shown here) and mid-tropospheric humidity were also poorly correlated to severe storms within regions of active convection. Wind shear and mid-level moisture are known to be related to severe storm occurrence. However, it is possible that the limitations upon the satellite soundings' vertical and horizontal resolution and absolute accuracy preclude a simple interpretation of severe storm potential from vertical variations in moisture and winds. Furthermore, our objective analysis itself may remove some small-scale details from these fields. Thus, the best predictors available from the group tested are the 50-kPa wind speed and 70-50 kPa temperature lapse rate.

The I_c estimates for the predictors in this particular forecasting problem are much lower than the values for the general thunderstorm predictors. These low values are reflected in the relative frequency histograms for the 50-kPa wind speed and for TLPS (Fig. 10). Neither predictor appears to be capable of indicating areas with storm potential much greater or lower than the sample's mean relative frequency of 6%, unless extremely high or low values of the predictors are encountered.

Given the nature of the sample which was available, the rarity of severe storm reports, and the errors introduced through the necessary use of radar observations to infer thunderstorm occurrence, these results must be considered preliminary. Note that the 95% confidence limit on the I_c for an uncorrelated predictor (.006) is significantly larger than the same confidence limit on predictors in the general thunderstorm forecasting experiment. The I_c values for several of the indices that were tested actually fell below this confidence limit.

Having more thunderstorm cases available would enable us to create probability tables with more predictors categories, and thus a better approximation to the true storm relative frequency distribution and I_c. Thus a larger data sample, especially one that included all of the active severe weather days, would probably yield estimates of greater predictive information for many of the indices tested. It should be remembered, however, that skill in statistical severe local storm prediction over a period of several hours is significantly lower than that in general thunderstorm prediction (RF, CH84).

9. COMPARISON AMONG INTERACTIVE PREDICTORS OF SEVERE LOCAL STORMS

Following the procedure used in the general thunderstorm forecasting experiment, we constructed severe storm relative frequency tables as a function of two variables. These two-way contingency tables feature only sixteen categories, in order to insure that at least 200 thunderstorm cases fell into each category. Again, our interest centered on predictor combinations in which the two predictors are not strongly correlated with each other. Various predictors were tested in combination with TLPS and the 50-kPa wind speed.

Values of I_c for the interactive predictors appear in Fig. 11. Most of the predictors have appeared earlier or are self-explanatory. In these tables, the climatic frequency is the percentage of thunderstorm days with severe local storms, estimated for each month and each MDR grid block on the basis of 1974-83 data. It was encouraging to note that the combination of TLPS and 50-kPa wind speed had a relatively high I_c, as would be expected from the single predictor experiment. This interactive predictor can delineate areas with conditional severe storm potential as high as 18% (see Fig. 12). The combination of climatic frequency and 50-kPa wind speed had a slightly lower maximum storm relative frequency but a higher I_c, because several categories had very low observed event frequency (Fig. 13). Again, these results must be accepted with caution, since the information ratios were obtained from a small data sample. Neverthless, the relationships illustrated by the interactive predictor tables appear reasonable and are physically supportable.

10. ASSESSMENT OF THE INFORMATION CONTENT OF TIME-CHANGE PREDICTORS IN SEVERE STORM FORECASTING.

Most researchers have concluded that satellite retrievals of atmospheric quantities possess only fair absolute accuracy relative to ground truth data. However, a number of studies have indicated that these retrievals should possess a useful degree of accuracy in representing spatial and temporal variations in stability and moisture (see, for example, Mostek et al., 1986). Therefore, we next turned our attention to an assessment of the relationships between the time rate of change of VAS-derived stability, wind, and moisture parameters, and subsequent severe convective storms.

Our dataset contained 50 days in which retrievals were available at 1100, 1400, and 1700 GMT together. Objective analyses were prepared from data at each of the observation times, and 3-h (1400-1700 GMT) and 6-h (1100-1700 GMT) time changes were computed at each grid block. The time changes were then examined for correlation to conditional severe storm occurrence during the 2000-0000 GMT period.

This data sample is already smaller than the one available for experiments with 1700 GMT data; furthermore a time change could not be computed if data were missing at either observation time. Thus, only 2940 thunderstorm cases were available for evaluation, including 170 severe storm cases. The I_c estimates presented later are based upon a six-category stratification of the predictors, with 490 cases in each category. While these results must again be accepted with caution, we believe that they are representative of the results that would have been obtained from a larger sample.

We examined the observed time rates of change of a number of variables held to be important in the development of the severe storm environment. These

include stability (MK and Showalter indices), low-level temperature (85-kPa temperature and skin temperature), wind speed, and mid-tropospheric relative humidity. To provide a basis for comparison with other time rate-of-change variables available to forecasters, changes in surface air temperature and terrain pressure were also considered.

The results of the comparison appear in Fig. 14. Note that the I_c values for 3-h and 6-h time changes were computed from slightly different data samples, and thus cannot be compared to each other with confidence. The basic result is the same: our data show very low correlations between storm occurrence and time changes in stability, wind, or moisture. Only the time-change in skin temperature appears to be correlated to intense convection, and then rather weakly. This variable is an estimate of the blackbody temperature of the earth's surface. During the retrieval process, it is initially estimated from the brightness temperatures in the "split window" water vapor channels 7 and 8 (Hayden, 1986). This estimate may be modified during the retrieval process.

The relative frequency histograms for skin temperature change (Fig. 15) shows a reasonable relationship between surface heating and subsequent severe weather. Within this sample of cases, time changes in skin temperature appear to be more strongly correlated to severe weather than are changes in surface air temperature.

We recognize that time rate-of-change information becomes "old" very quickly. It is possible that our disappointingly low estimates of I_c are due to the fact that 3 hours elapse between the second observation time and the start of the verification period; this interval may be outside the temporal range of influence. To test this hypothesis, new values of I_c with respect to storm events during the period 1800-2200 GMT were estimated. Thus a much shorter lead time was assumed. However, the results were similar to those obtained before. While users of VAS data have noted apparent relationships between humidity and stability trends and subsequent convection, it seems that the magnitude of these changes is not consistently related to severe storm relative frequency. Even the relative frequency histogram for skin temperature change shows a rather weak, though recognizeable, relationship. We hope to continue these experiments as more VAS data become available.

11. EVALUATION OF THE EFFECT OF UPDATING UPON THE PREDICTIVE INFORMATION WITHIN STABILITY INDICES

Severe convective storms often develop in situations in which stability, humidity, and winds change rapidly in time. The existing operational upper-air network supplies regular observations only at 12-h intervals. Even then, over the United States these observations are taken during local morning and evening; thus upper-air observations of the well-mixed preconvective atmosphere are usually not available. It has long been hoped that sounders aboard geostationary satellites might act to fill in this particular observational gap.

One of our aims was exploring the diurnal changes in the relationships between some of the predictors described earlier and convective activity. Observations taken at 1100, 1400, and 1700 GMT were used in calculating TLPS, 50-kPa windspeed, and the MK index. We then correlated the indices from each observation time to thunderstorm occurrence during the 2000-0000 GMT period. As in our experiments with rate-of-change predictors, 50 days of observations were available.

Our purpose here was documenting the manner in which the I_c of these predictors changes as the basic observational information is updated. In computing estimates of I_c for the indices derived from the different sets of observations, precisely matched data samples were used. If VAS observations for a grid block were missing at one time, that case was eliminated from consideration at the other two times as well.

Table 1 shows our estimates of I_c for the MK index with respect to thunderstorms, and for TLPS and 50-kPa wind speed with respect to severe local storms. These figures confirm our belief that predictive information should increase as the observations are taken closer to the verification period. However, we noted that I_c does not increase consistently between 1100 and 1400 GMT, or from 1400 to 1700 GMT. The changes in I_c are not large, and the event relative frequency histograms do not change radically from one period to the next. As an illustration, Fig. 16 shows the thunderstorm relative frequency distribution for both the 1100 and 1700 GMT MK index. The category dividers for the two distributions are not identical; the 1100 and 1700 MK indices are distributed differently, making it necessary to select slightly different dividers in order to insure that equal numbers of cases fell into each category. The 1700 GMT dividers are shown as abscissae for reference.

The frequency curve for 1700 GMT indicates slightly greater information; this may be inferred since the 1700 GMT curve is lower than the 1100 GMT curve for MK values less than 28°C, but higher than the 1100 GMT curve for MK greater than 44°C. To assess the statistical significance of the differences between the two curves, a chi-squared statistic was computed between the storm absolute frequency distributions used in developing the relative frequency curves. This test indicated that the differences are significant at the 95% confidence level. There are, however, no large systematic differences between the two distributions. This indicates that the two predictors have almost the same information content, suggesting that VAS retrievals with even shorter lead times may be required to significantly improve the correlation between stability indices and thunderstorm occurrence.

The severe local storm relative frequency as a function of 50-kPa wind speed appears in a similar illustration (Fig. 17). In this graph, the frequency distribution between the endpoint values was lightly smoothed to remove oscillations that make the comparison difficult. As in Fig. 16, the frequency curve for the 1700 GMT predictor shows greater information than does the 1100 GMT curve, but the differences between the distributions are small.

We suspect that there should be a consistent increase in information as the observations are updated from 1100 to 1400 GMT, and again updated at 1700 GMT. The apparent inconsistency in our results may be due in part to the small data sample we had available (only 20,000 cases for the general thunderstorm experiment, and 2800 thunderstorm cases for the severe storm experiment). Yet the present results could also suggest that the stability and wind information must be updated more frequently (every 1 to 2 h) if any substantial benefit is to be gained in this forecasting context.

Though it seems that the selected updating interval has little effect on predictive information, it should be remembered that we consider all cases at once in computing our estimates of I_c. It is logical to expect that updated stability observations would have the greatest positive impact during rapidly-evolving severe weather situations. Our data sample consists primarily of

rather quiet convection days, particularly during the generally active months of March and April. On days with significant severe weather, VAS operations were often interrupted to allow for VISSR rapid-interval scanning. Because of this deficiency in the available experimental data, we can not be certain, at this time, that updated VAS stability observations of 3- and 6-h lead time would be of little value in all circumstances.

12. EFFECTS OF HORIZONTAL SMOOTHING OF PREDICTOR FIELDS UPON THEIR INFORMATION CONTENT

In order to carry out our comparisons between VAS-derived indices and convective weather events, we first had to objectively interpolate the index values from randomly-distributed VAS retrieval locations to the MDR archive grid. We used a version of the Barnes (1964, 1973) objective analysis scheme to carry out the interpolation. The Barnes scheme, like others, treats data values at map grid points as the weighted average of the observations in some nearby region. Observations closer to the grid point generally receive greater weight in the average than do observations farther away. In the Barnes scheme, the weights decrease as the exponential of the square of the distance between the observation and the grid point. A correction may then be made to the initial estimates so that there is better agreement between the interpolated field and the original observations. We employed a version of this two-pass Barnes algorithm in deriving our predictor fields.

Changes in the exact shape of the weighting function and in the number of correction passes used will, of course, affect the final data field. If the weighting function is designed so that weight decreases very sharply with distance, or if more than two corrective passes are made, short-wavelength features in the data field will have more amplitude. We arbitrarily selected a set of weighting parameters that produced a smoothly-varying field with good agreement to the original observations. Since changes in the objective analysis affect the variance of the interpolated field, tests were conducted to determine how much the estimates of I_c might change when different analysis schemes were used in making the estimates.

Two new analyses of the SK index, TLPS, and 50-kPa wind speed fields were prepared. One analysis was simply the one-pass first guess to the fields used in our experiments. This is a relatively "smooth" analysis with little amplitude in short wavelengths. In the other, a third pass was incorporated to force better agreement between analyses and observations. Thus, one new analysis featured less variance than the original two-pass version; the other new analysis featured more variance. Estimates of I_c with respect to thunderstorms and with respect to severe storms were then made with the new analyses.

Table 2 shows predictor variance and estimates of I_c for each of the three analyses. Some differences will be noted between the figures shown here and those appearing in Figs. 1 and 9 because slightly different data samples were used in preparing them. It can be seen that the "smoother" one- and two-pass analyses yield larger values of I_c than the three-pass analyses did. These results are consistent with earlier findings by RF, CH84 and Kitzmiller (1985), who found that moderate horizontal smoothing on these scales tends to increase the linear correlation between stability indices and thunderstorm occurrence. However, the changes in I_c and in the corresponding relative frequency distributions are not large. We conclude that our estimates of I_c are not greatly affected by changes in the objective analysis scheme.

It might seem that the three-pass analyses, with their greater horizontal detail, should yield the greatest predictive information. It must be remembered that virtually all correlation measures, including the I_c, depend upon both the predictor/predictand covariance and the predictor variance. The linear correlation coefficient itself depends upon the ratio of the predictor/predictand covariance to the predictor standard deviation (see, for example, Panofsky and Brier, 1968). A closer examinination of our results showed that the three-pass analyses had the largest covariance between the predictors and storm occurrence, as we might expect. However, the predictor variance was also relatively large. The net result was a lower correlation coefficient and I_c. In other words, the three-pass analyses possess not only greater amplitude in the features associated with storm potential, but greater amplitude in irrelevant features, as well. Thus, there is a net loss of predictive information. Since out dataset is relatively small and results obtained here might not extend to other data samples, we did not attempt to find an objective analysis scheme that optimized the I_c.

13. COMPARISON BETWEEN PREDICTORS DERIVED FROM VAS PRODUCTS AND FROM LFM ANALYSES AND FORECASTS

In practice, two sources of upper-air data are already available to forecasters: rawindsondes and numerically-produced forecasts. These data are commonly used in conjuction with hourly surface observations to produce updated stability estimates (see, for example, CH84 and Bothwell et al., 1985). The VAS retrievals, which incorporate surface observations, a numerical forecast for first-guess temperature and dew point profiles, and irradiance measurements, represent a logical extension of the existing observational system to include new physical data.

Our primary purpose in this study was to demonstrate the optimum manner in which VAS could be used to supplement and improve upon observational systems that are currently operational. Therefore, several experiments were carried out to demonstrate the relative strengths of numerical forecasts, raobs, and VAS products in convection forecasting applications. This was done by comparing values of I_c estimated for the same predictors when they were derived from VAS retrievals and from concurrently-available raobs and Limited-area Fine Mesh (LFM) model (Gerrity, 1977) forecasts.

The vertical structure of the retrieved temperature and moisture profiles already depend in part upon the LFM forecast that was used to supply the first guess. During the 1984-85 assessment experiments, this forecast was a 12- or 24-h projection from the model run initiated at 0000 GMT. An analysis of hourly surface observations of temperature, humidity, and terrain pressure were used to provide the first guess at the surface level; the retrieval process does not alter the observed values.

Since the upper-air portion of the first guess is available well before the satellite irradiance measurements, we wished to know how much additional predictive information is added by the retrieval process. We therefore prepared separate sets of objective analyses of K index computed once with the guess temperature and dew point, and again with the retrieved values. The K values were then correlated to thunderstorm observations. The first guess for each profile was included with the retrievals; the guess and retrieval analyses were prepared in precisely the same manner. The K index, rather than the SK or MK indices, was used here because K does not include surface-level data, which is identical in the retrieval and guess.

Thunderstorm relative frequency during the 2000-0000 GMT period is shown as a function of 1700 GMT retrieval and guess K in Fig. 18. The predictor category dividers shown are for the retrieval K index. While there are small differences between the two curves, we did find that the retrieval K yielded an I_c of 0.24 while the guess K yielded one of 0.23. A chi-squared test showed the differences between the two distributions to be significant at the 95% confidence level. While the differences in the two frequency distributions alone do not prove that the retrieval has better stability information than the guess, it is encouraging to find that the data sample under consideration gave a positive result.

By the time 1700 GMT VAS retrievals are processed, morning raobs and 1200 GMT LFM forecasts are available at all routine dissemination points. Another set of experiments was carried out to determine if the VAS products possess more predictive information than the latter two sources. We extracted from TDL archives the 1200 GMT LFM initial fields and 12-h forecasts made on 73 days on which 1700 GMT VAS data were also processed. While we considered preparing objective analyses of stability predictors from individual radiosonde observations, we chose to use the available LFM initial fields, instead. Though these initial fields might lack some of the horizontal and vertical details that could be better resolved in other objective analyses, we felt that the LFM product was sufficiently representative of raob analyses for our purposes. No analysis based upon radiosonde observations can fully resolve features below the subsynoptic scale, because of the observing network's spacing; furthermore, as noted in Section 12, information on general thunderstorm potential does not appear to be enhanced by attempting to account for the amplitude of the smallest analyzed features in the stability field. We thus felt that the LFM initial fields would be an adequate representation of radiosonde analyses for our VAS/raob comparison. In this way we also could more readily compare differences in the information content between these analyses and subsequent LFM forecasts.

Values of the SK index, 50-kPa wind speed, and TLPS were computed from the LFM data and interpolated to the MDR grid. Estimates of I_c with respect to thunderstorms and severe local storms were then made for the predictors as derived from each of the three data sources; as before, we employed a verification period of 2000-0000 GMT. Cloud gaps within the VAS analyses were eliminated from consideration entirely, so that the various I_c estimates were made from a precisely matched sample of cases.

From the results shown in Table 3, it appears that the 1700 GMT VAS data provide more information than the 1200 GMT upper-air analyses, a result obtained in a comparison made with polar-orbiter satellite soundings by Keller and Smith (1983). However, VAS appears to yield slightly less information than the 12-h LFM forecast verifying at 0000 GMT. The differences in information are small, as may be inferred from the relative frequency distributions for VAS- and LFM-derived predictors shown in Figs. 19 and 20. Here, the relative frequency curves defined by 1700 GMT VAS and 12-h LFM forecasted predictors appear together. Because the VAS and LFM predictors are distributed differently, the category dividers for the two sets of predictors are not identical; the dividers for the VAS predictors are shown for reference. For thunderstorm frequency (Fig. 19) and for severe storm frequency as a function of 50-kPa wind speed (Fig. 20a), the distributions differ only slightly. There are somewhat larger differences in the two distributions for the TLPS predictor (Fig. 20b). From these relative frequency distributions, we conclude that there are in fact only

small differences in the information content between VAS predictors and concurrently-available LFM forecasts.

It must be noted again that the VAS retrievals made during 1984 and 1985 employed forecasts from the 0000 GMT LFM run for the first-guess profiles. In practice, the retrieval algorithm rarely changes the first guess to any great extent; thus the final retrievals are almost surely affected when the LFM forecast is poor. It would have been preferable to use forecasts based upon 1200 GMT raob information in the first guess, but constraints on communications between the VAS processing facility and the National Meteorological Center prevented this.

Moreover, the LFM analyses and forecasts have a smaller variance than the VAS analyses do. As noted in our discussion of the effects of the objective analysis scheme, this alone could account for the LFM predictors' larger correlation to storm occurrence.

While it seems that the LFM-derived predictors possess more information than ones derived from VAS, it should be recalled that we base this conclusion on values of I_c computed from the entire data sample. Our approach shows which indices bear the most persistent relationship to storm potential over a wide variety of situations. This is precisely what we need to know in developing a system for providing objective probabilistic guidance. Forecasters making a subjective interpretation of the convective potential might find that satellite retrievals yield a "better" representation of the stability field than a model forecast does, since the retrievals possess more spatial details. However, the presence of such detail evidently does not always increase the amount of information when the stability/storm potential relationship is examined over many cases.

When a larger data sample becomes available, a more sophisticated comparison between VAS and the LFM model or the Nested Grid Model (Phillips, 1979; Hoke, 1984), involving a forecast and verification experiment, will be undertaken.

14. SUMMARY AND CONCLUSIONS

An extensive series of experiments have been carried out to show the potential that a number of VAS products have as predictors of thunderstorm and severe local storm activity. In these experiments, several stability and moisture parameters were computed from VAS retrievals and correlated to subsequent storm occurrences. All available VAS retrievals processed semi-operationally over the United States during the spring and summer of 1984-85 were used.

Our first experiments demonstrated the relative predictive value of a number of stability indices. The indices were computed from VAS retrievals made from 1700 GMT measurements, then compared to thunderstorm and severe local storm observations during the subsequent 2000-0000 GMT period. The computed information ratio (I_c) was used as a measure of the correlation between the magnitude of the stability indices and the observed relative frequency of storm events.

We found that versions of the K index modified to include surface temperature

and dew point had the largest value of I_c among a group of general thunderstorm predictors. Consideration of low-level negative buoyant energy along with the modified K index added some information. For discriminating severe local storm cases from general thunderstorm cases, the 70-50 kPa temperature lapse rate and the 50-kPa gradient wind speed had the greatest predictive information. An interactive predictor that incorporated both these indices had significantly greater information than either one considered alone.

The relationships between the 3-h and 6-h time changes of several variables and subsequent severe local storm relative frequency were also examined. The changes in most variables were only poorly correlated to storm events. Of the variables tested, only the change in skin (surface blackbody) temperature possessed any predictive information.

Next, the effects of updating upon the I_c of several VAS-derived indices were documented. The SK index, lapse rate, and 50-kPa wind speed were computed from retrievals made at 1100, 1400, and 1700 GMT. The values of I_c with respect to thunderstorm and severe local storm occurrence were then computed. It was found that predictive information increased slightly as the VAS observation time approached the 2000-0000 GMT storm observation period.

Finally, the predictive value of VAS-derived indices was compared to that of the same indices when derived from concurrently-available raobs and LFM forecasts valid near the storm observation period. The 1200 GMT LFM initial field was used as a representative raob analysis, while the retrieval first guess and the 12-h LFM forecast valid at 0000 GMT provided the numerically-forecasted temperature and humidity data. Our results suggest that the 1700 GMT VAS retrievals possess more information on storm potential than do 1200 GMT raobs, but less information.than does the 12-h LFM forecast. The retrievals seem to yield more information than do their own first guess profiles.

While our results indicate that VAS could add little to operational statistical thunderstorm forecasting techniques, we must point out that retrieval operations during 1984 and 1985 were carried out under less-than-ideal conditions. First, the daytime retrievals were prepared without the most up-to-date raobs (those taken at 1200 GMT) as a first guess. When processing operations at the new World Weather Building VAS Data Utilization Center are carried out as planned, these observations will be available, and the accuracy of the soundings should improve. Also, constraints on the useage of GOES prevented VAS operations on many active storm days, when timely updates of stability information would have been most helpful. When two GOES satellites are in full operation, and when the retrieval process is fully automated, many more sounding datasets should be available for study. This study could therefore be regarded as a baseline with which to compare future VAS systems.

On the basis of our results, we now suspect that modest improvements in remote soundings of the atmosphere might not necessarily lead to better objective convection forecasts. It was noted earlier that LFM stability forecasts, which have limited subsynoptic detail, provide at least as much predictive information as updated VAS retrievals. This finding illustrates a basic problem in forecasting the occurrence of convective phenomena: moisture and stability alone do not determine precisely where in an unstable air mass thunderstorms will break out. We may judge the convective potential over a fairly large area from the K or lifted indices; however, if we are to pinpoint locations of storm development within that area we must also determine where low-level air

confluence is taking place and initiating convection. In addition to potential instability, small-scale dynamic features such as convergence lines and thunderstorm outflow boundaries are of prime importance in initiating deep convection. Wind observations from the Next Generation Radar system could therefore be highly useful in approaching this forecasting problem.

It is true that important convergence features are often reflected in the humidity or stability fields, as in dryline situations. Satellite observations easily resolve such phenomena, but surface observations do so as well. Soundings with improved vertical detail could possibly show where convergence was acting to break down capping inversions. However, present satellite sounding systems cannot consistently resolve such vertical details. In most cases with weak synoptic-scale forcing, low-level confluence may be evident only in the wind field or where visible satellite imagery shows developing cumulus.

Thus, moderately improved temperature and moisture soundings alone cannot be expected to provide all of the information needed to prepare good convection forecasts. As noted by Stone (1985), observations of air motion are also necessary.

Forecasters at NSSFC, where VAS data have been available in near real time since 1982, now rely on VAS mainly to provide better guidance on the location of synoptic-scale features and air mass boundaries, rather than absolute values of stability (Shoeni and Mosher, 1986). For example, 6.7 μ imagery is often used to track the movement of upper-level moisture features associated with the jet stream. High-resolution (60-km) color-enhanced images of retrieved precipitable water and lifted index are animated to show the movement of low-level moisture. These guidance products make use of VAS data's best characteristics, its high horizontal resolution and acceptable relative accuracy.

On the basis of our experimental results, we believe that future research should emphasize applications of the observations that only a satellite can provide, such as skin temperature and upper-level winds derived from cloud or moisture tracking. Satellite sounders provide a large quantity of information on the atmospheric state, but we are only beginning to understand how to make the best use of this information. Multichannel satellite observations of the earth and atmosphere could well become a keystone of our weather forecasting operations. However, further efforts will be required to show how these satellite observing systems can be most effectively utilized in future forecasting operations.

ACKNOWLEDGEMENTS

In the course of this research, we received help from many people in NESDIS and NWS. We wish to thank Dr. W. Paul Menzel and Messrs. Roney Sorenson, Geary Callan, Anthony Seibers, and Gary Wade at the ASPP for providing the VAS retrievals, answering dozens of questions, and reviewing this manuscript. Mr. Frederick Mosher provided us with some of the early results of VAS assessment at NSSFC. Mr. Henry Robinson, National Weather Service Office of Meteorology, supplied the code for a version of the one-dimensional cumulus model. Dr. Dennis Chesters at NASA/GLA reviewed the manuscript and gave us valuable advice on its content. Dr. Jerome Charba gave us advice on the conduct of the experiments and kindly provided the surface data analyses. We would like to thank Dr. Harry Glahn for reviewing this work and providing valuable suggestions on the interpretation of results. Mrs. Belinda Howard prepared the final version of the manuscript.

REFERENCES

Anthony, R. W., and G. S. Wade, 1983: VAS operational assessment findings for spring 1982-83. Preprints 13th Conference on Severe Local Storms, Tulsa, Amer. Meteor. Soc., Boston, J23-28.

_____, and P. W. Leftwich, Jr., 1984: Operational VAS applications in identifying regions with potential for severe thunderstorm development. Preprints 10th Conference on Weather Forecasting and Analysis, Clearwater Beach, Amer. Meteor. Soc., Boston, 358-364.

Barnes, S. L., 1964: A technique for maximizing details in numerical weather map analysis. J. Appl. Meteor., 3, 396-409.

_____, 1973: Objective map analysis using weighted time-series observations. NOAA Technical Memorandum ERL NSSL-62, National Oceanic and Atmospheric Administration, U.S. Department of Commerce, 60 pp.

Bothwell, P. D., R. A. Maddox, C. A. Doswell, III, and K. C. Crawford, 1984: Operational methods for increasing the reliability of information derived from conventional surface and upper air data. Preprints 14th Conference on Severe Local Storms, Indianapolis, Amer. Meteor. Soc., Boston, 402-405.

Charba, J. P., 1979: Two-six hour severe local storm probabilities: An operational forecasting system. Mon. Wea. Rev., 107, 268-282.

_____, 1984: Two-to-six hour probabilities of thunderstorms and severe local storms. NWS Technical Procedures Bulletin No. 342, National Oceanic and Atmospheric Administration, U.S. Department of Commerce, 14 pp.

Crum, T. D., and J. J. Cahir, 1983: Experiments in shower-top forecasting using an interactive one-dimensional cloud model. Mon. Wea. Rev., 111, 829-835.

Doswell, C. A., III, F. Caracena, and M. Magnagno, 1985: Temporal evolution of 700-500 mb lapse rate as a forecasting tool--a case study. Preprints 14th Conference on Severe Local Storms, Indianapolis, Amer. Meteor. Soc., Boston, 398-401.

Galway, J. G., 1956: The lifted index as a predictor of latent instability. Bull. Amer. Meteor. Soc., 37, 528-529.

George, J. J., 1960: Weather Forecasting for Aeronautics. Academic Press, 673 pp.

Gerrity, J. F., 1977: The LFM model - 1976: A documentation. NOAA Technical Memorandum NWS NMC-60, National Oceanic and Atmospheric Administration, U.S. Department of Commerce, 68 pp. [NTIS P13 279 419/6].

Hayden, C. M., 1986: Proposed filter changes for the GOES-NEXT sounder--the role of surface skin temperature in the current VAS algorithm. Memorandum for the record dated 23 January, 1986, National Oceanic and Atmospheric Administration, U.S. Department of Commerce, 12 pp.

Hoke, J. E., 1984: Forecast results for NMC's new Regional Analysis and Forecast System. Preprints 10th Conference on Weather Forecasting and Analysis, Clearwater Beach, Amer. Meteor. Soc., Boston, 418-423.

Holloway, J. L., and M. A. Woodbury, 1955: Application of information theory and discriminant function analysis to weather forecasting and forecast verification. Technical Report 1, Contract No. 551(07), Institute for Cooperative Studies, University of Pennsylvania, Philadelphia, 85 pp.

Keller, D. L., and W. L. Smith, 1983: A statistical technique for forecasting severe weather from vertical soundings by satellite and radiosonde. NOAA Technical Report NESDIS 5, National Oceanic and Atmospheric Administration, U.S. Department of Commerce, 35 pp.

Kitzmiller, D. H., 1985: The application of cumulus models to MOS forecasts of convective weather. NOAA Technical Memorandum NWS TDL 76, National Oceanic and Atmospheric Administration, U.S. Department of Commerce, 50 pp.

Livingston, R. L., and G. L. Darkow, 1979: Subsynoptic variability in the pretornado environment. Preprints 11th Conference on Severe Local Storms, Kansas City, Amer. Meteor. Soc., Boston, 114-121.

Lund, I. A., and E. W. Wahl, 1955: An objective system for preparing operational weather forecasts. Air Force Surveys in Geophysics No. AFCRCTN-55-219, Air Force Cambridge Research Center, Bedford, Massachusetts, 7 pp.

Menzel, W. P., and A. J. Schreiner, 1985: Effects of filter wheel temperature excursions on VAS radiative transfer calculations. Memorandum for the record dated 30 April, 1985, National Oceanic and Atmospheric Administration, U.S. Department of Commerce, 8 pp.

Miller, R. C., 1972: Notes on analysis and severe weather forecasting procedures of the Air Force Global Weather Center. Air Weather Service Tech. Rep. 200 (Rev.), U.S. Air Force, 102 pp. [NTIS AD 744 042].

Mostek, A., L. W. Ucellini, R. A. Petersen, and D. Chesters, 1986: Assessment of VAS soundings in the analysis of a preconvective environment. Mon. Wea. Rev., 114, 62-87.

Panofsky, H. A., and G. W. Brier, 1965: Some Applications of Statistics to Meteorology. The Pennsylvania State University, University Park, 224 pp.

Phillips, N. A., 1979: The nested grid model. NOAA Technical Report NWS 22, National Oceanic and Atmospheric Administration, U.S. Department of Commerce, 80 pp.

Purdom, J. F. W., 1985: The application of satellite sounding and image data to the Carolina tornado outbreak of 28 March 1984. Preprints 14th Conference on Severe Local Storms, Indianapolis, Amer. Meteor. Soc., Boston, 276-279.

Reap, R. M., and D. S. Foster, 1979: Automated 12-36 hour probability forecasts of thunderstorms and severe local storms. J. Appl. Meteor., 18, 1304-1315.

Sanders, F., and A. J. Garrett, 1975: Application of a convective plume model to prediction of thunderstorms. Mon. Wea. Rev., 103, 874-877.

Shoeni, T. R., and F. R. Mosher, 1986: Real time use of VAS data at the National Severe Storms Forecast Center during 1985. Preprints 11th Conference on Weather Forecasting and Analysis, Kansas City, Amer. Meteor. Soc., Boston, 411-415.

Showalter, A. K., 1953: A stability index for thunderstorm forecasting. Bull. Amer. Meteor. Soc., 34, 250-252.

Simpson, J., and V. Wiggert, 1969: Models of precipitating cumulus towers. Mon. Wea. Rev., 97, 471-489.

Smith, W. L., V. E. Suomi, W. P. Menzel, H. M. Woolf, L. A. Sromovsky, H. E. Revercomb, C. M. Hayden, D. N. Erickson, and F. R. Mosher, 1981: First sounding results from VAS-D. Bull. Amer. Meteor. Soc., 62, 232-236.

_____, and H. M. Woolf, 1984: Improved vertical soundings from an amalgamation of polar and geostationary radiance observations. Preprints Conference on Satellite Meteorology/Remote Sensing and Applications, Clearwater Beach, Amer. Meteor. Soc., Boston, 45-48.

Stone, H. M., 1985: A comparison among various thermodynamic parameters for the prediction of convective activity: Part II. NOAA Technical Memorandum NWS ER-69, National Oceanic and Atmospheric Administration, U.S. Department of Commerce, 14 pp.

Wade, G. S., A. L. Siebers, and R. W. Anthony, 1985: An examination of current atmospheric stability and moisture products retrieved from VAS measurements in real time for the NSSFC. Preprints 14th Conference on Severe Local Storms, Indianapolis, Amer. Meteor. Soc., Boston, 105-108.

Table 1. Effect of updating on I_c. Values of I_c for MK index are with respect to general thunderstorm occurrence; values of I_c for TLPS and 50-kPa wind speed are with respect to conditional severe local storm occurrence. Verification period is 2000-0000 GMT.

Predictor	I_c for predictor derived from VAS retrievals made at: 1100 GMT	1400 GMT	1700 GMT
MK index	0.25	0.28	0.28
TLPS	0.18	0.18	0.25
50-kPa wind speed	0.36	0.28	0.40

Table 2. Values of I_c and predictor standard deviation for three different objective analyses. I_c for SK index is with respect to general thunderstorm occurrence; I_c for TLPS and 50-kPa wind speed is with respect to severe local storm occurrence. Predictors are computed from 1700 GMT VAS retrievals; verification period is 2000-0000 GMT.

Predictor	Standard deviation	Ic
1-pass SK index	12.4	0.29
2-pass SK index	13.1	0.28
3-pass SK index	13.2	0.28
1-pass TLPS	6.4	0.30
2-pass TLPS	7.1	0.27
3-pass TLPS	7.3	0.26
1-pass 50-kPa wind speed	7.5	0.41
2-pass 50-kPa wind speed	8.1	0.38
3-pass 50-kPa wind speed	8.2	0.37

Table 3. Comparison of I_c for predictors derived from 1700 GMT VAS retrievals, 1200 GMT LFM initial fields, and 12-h LFM forecasts valid at 0000 GMT. Verification period is 2000-0000 GMT.

Predictor	I_c
SK index derived from:	(with respect to general thunderstorm occurrence)
1700 GMT VAS	0.28
1200 GMT LFM Analysis	0.24
12-h LFM Forecast	0.30
TLPS derived from:	(with respect to severe local storm occurrence)
1700 GMT VAS	0.27
1200 GMT LFM Analysis	0.32
12-h LFM Forecast	0.37
50-kPa wind speed derived from:	
1700 GMT VAS	0.37
1200 GMT LFM Analysis	0.31
12-h LFM Forecast	0.36

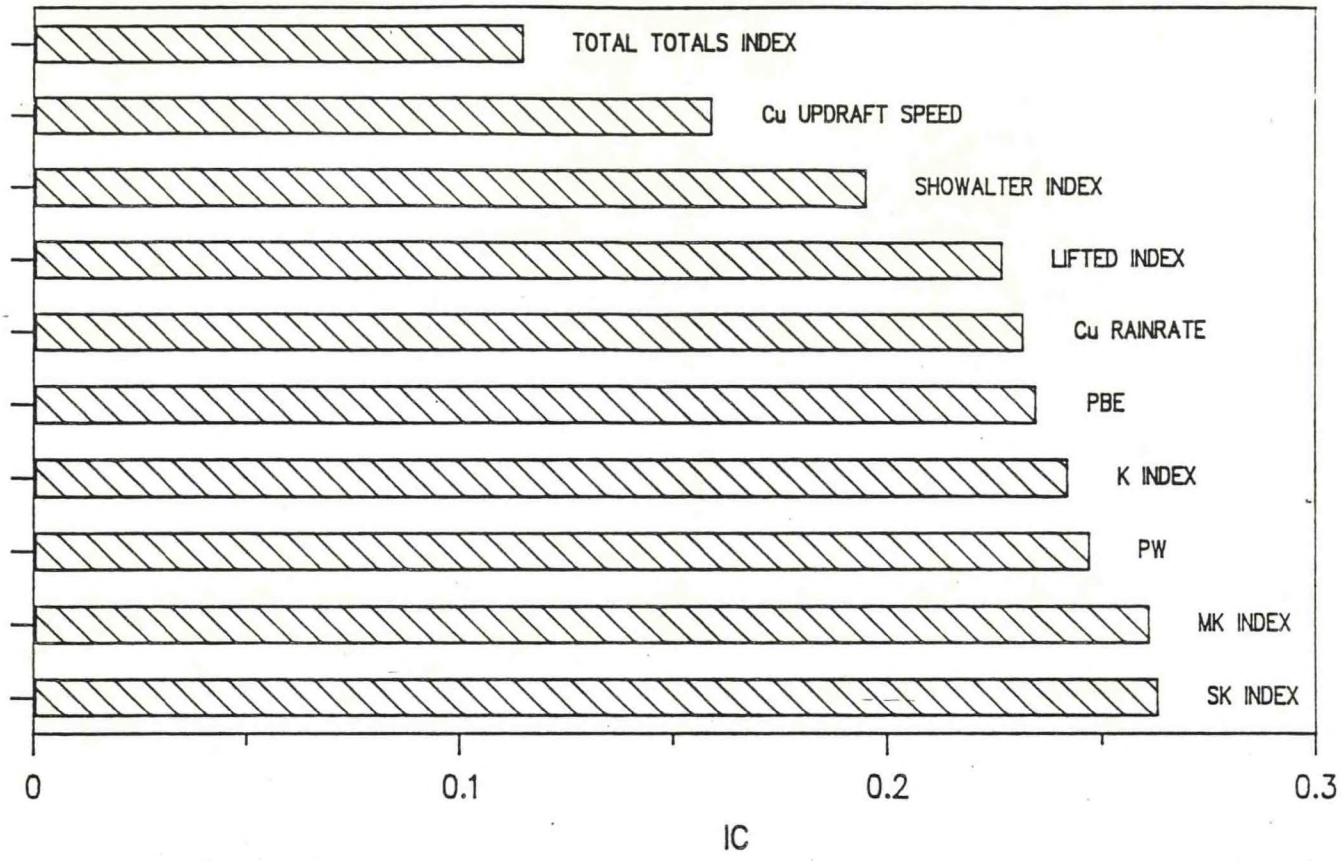

Figure 1. Computed information ratio (I_c) with respect to general thunderstorm occurrence for various predictors. Predictors are derived from 1700 GMT VAS retrievals; definitions found in the text. Thunderstorm observation period is 2000-0000 GMT.

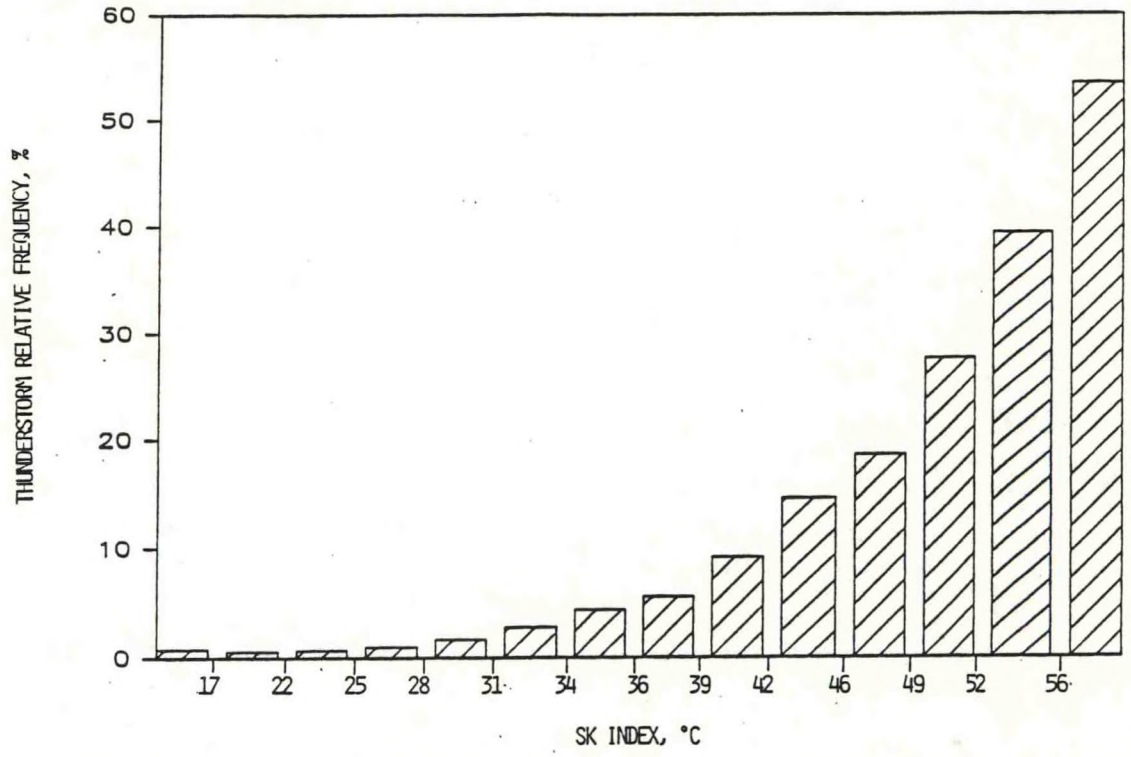

Figure 2. Observed thunderstorm relative frequency as a function of SK index. Thunderstorm events occurred during the period 2000-0000 GMT; SK index derived from 1700 GMT VAS retrievals. Each category contains approximately 2200 cases.

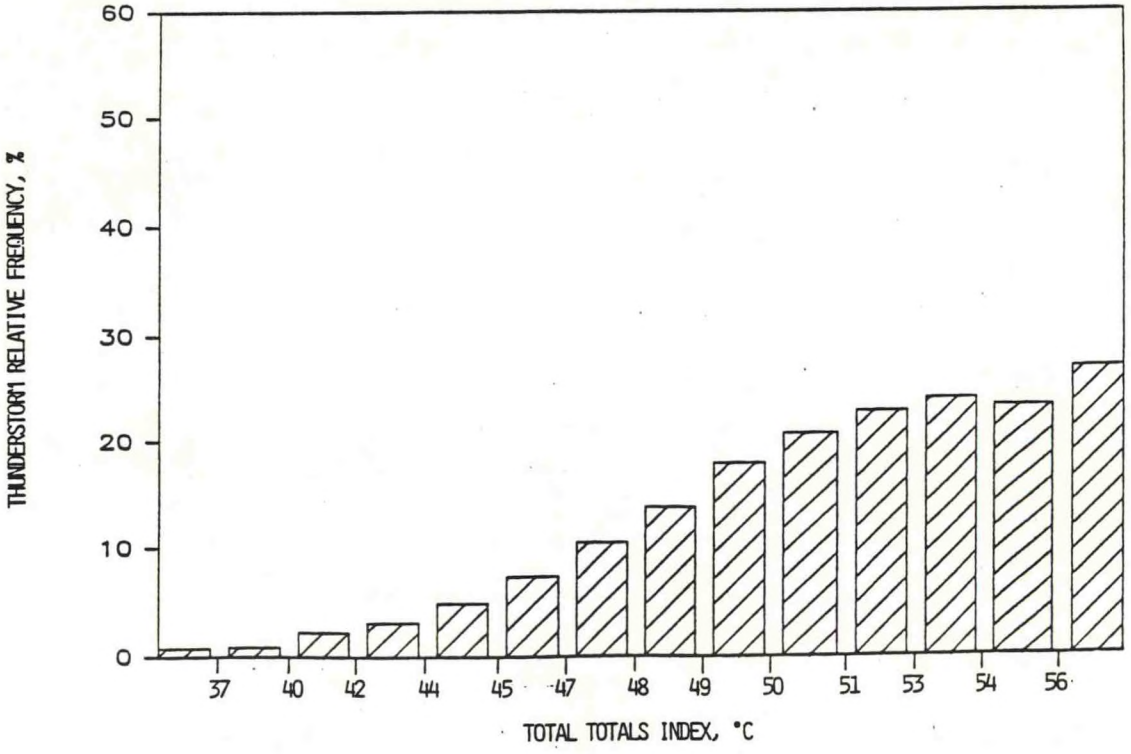

Figure 3. As in Fig. 2, except predictor is Total Totals index.

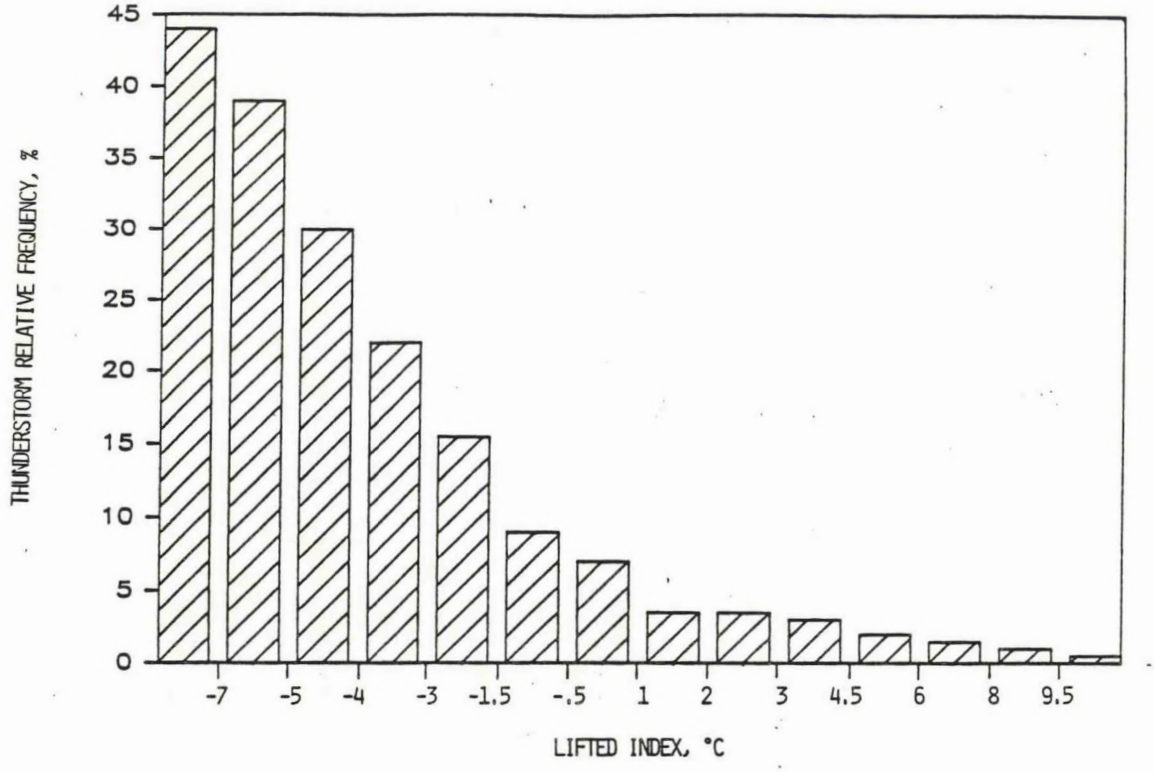

Figure 4. As in Fig. 2, except predictor is surface lifted index (LI).

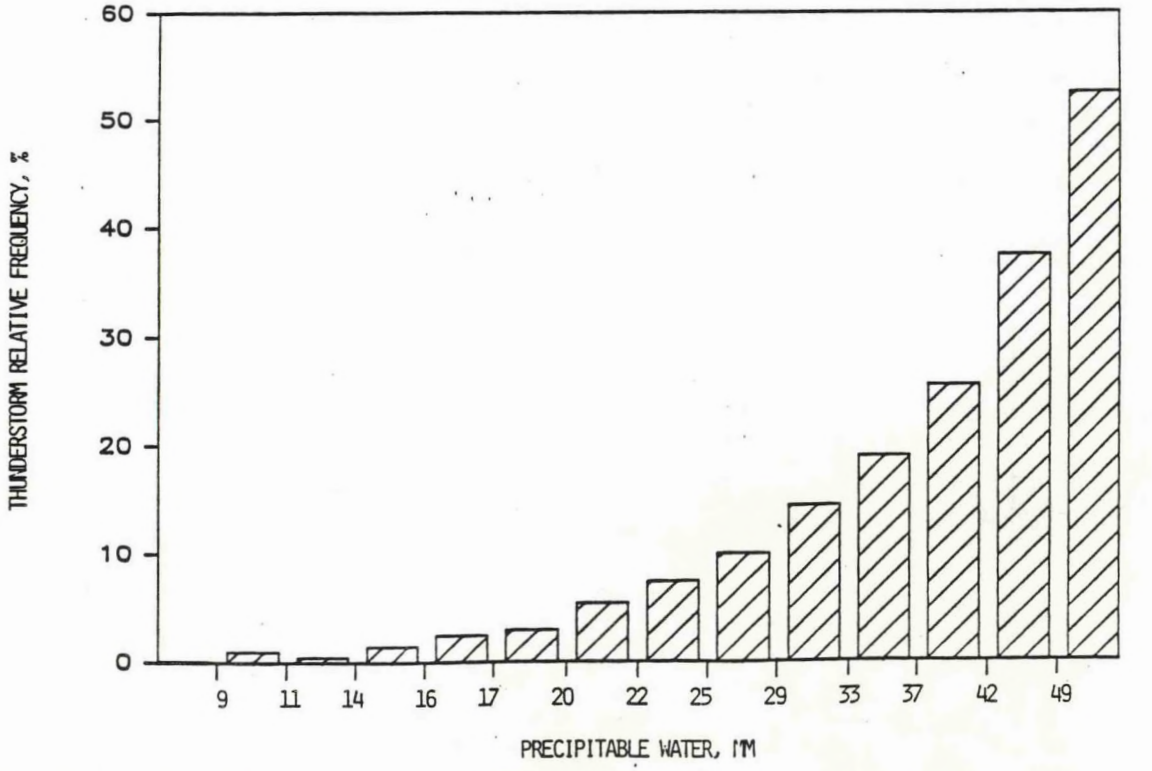

Figure 5. As in Fig. 1, except predictor is precipitable water (PW).

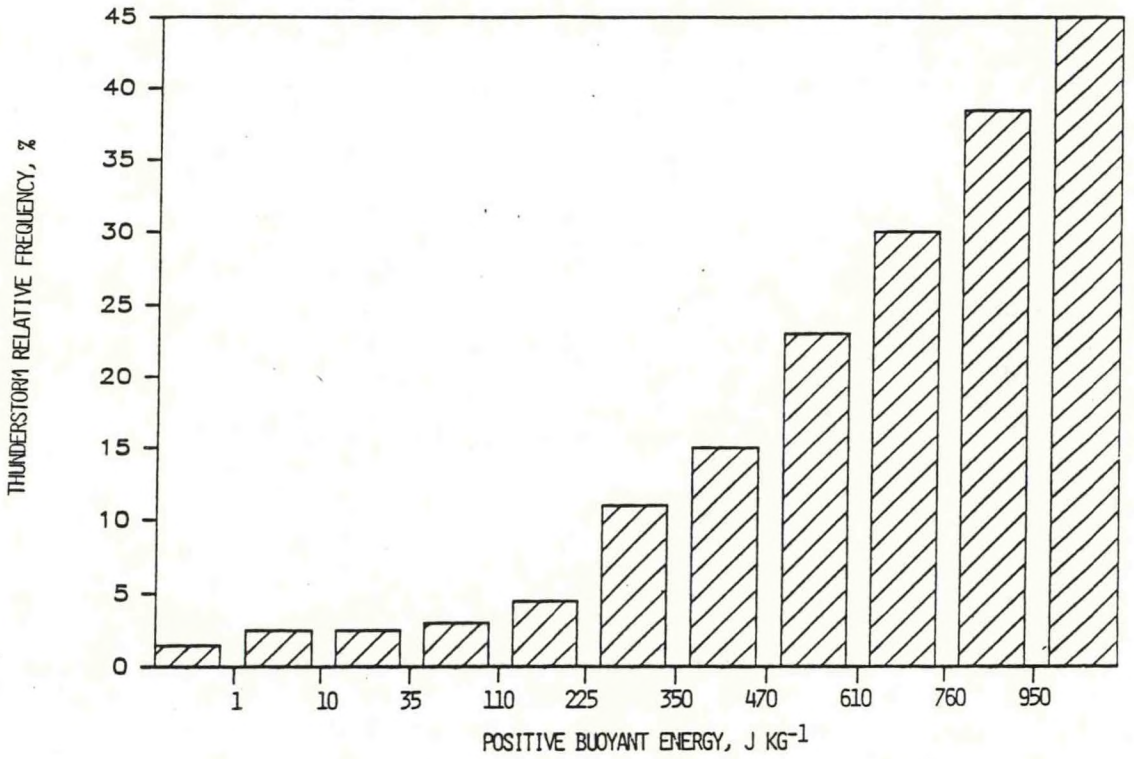

Figure 6. As in Fig. 1, except predictor is positive buoyant energy (PBE).

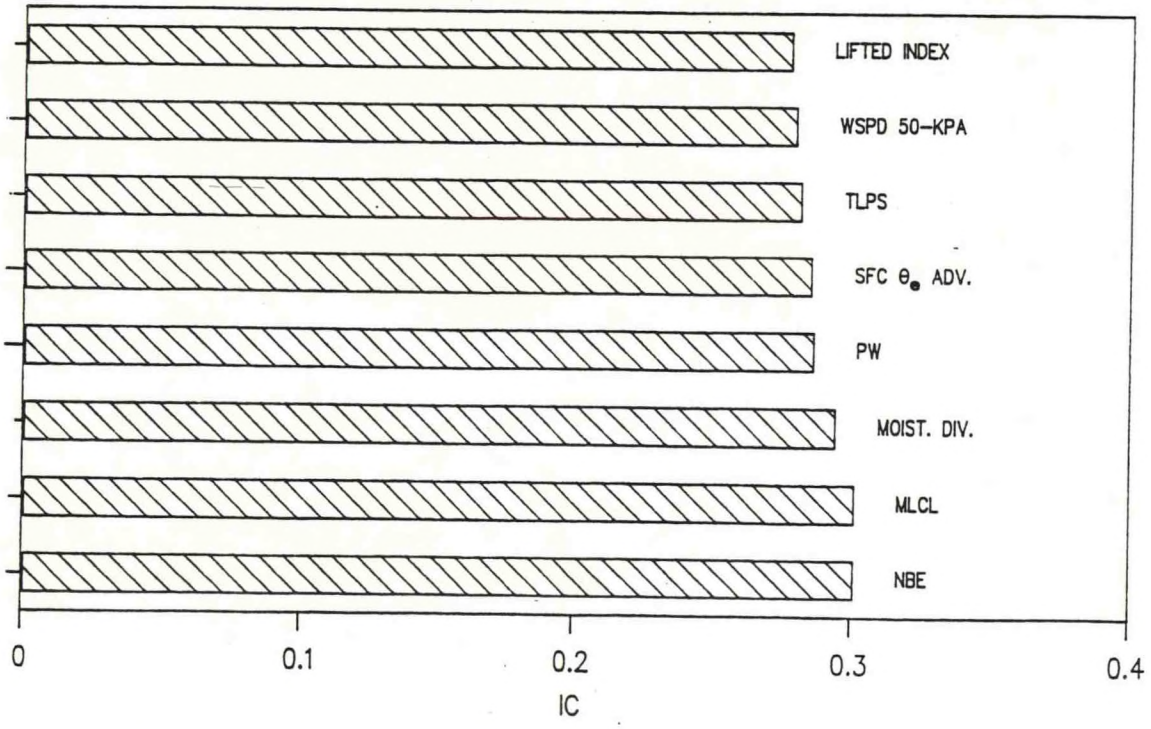

Figure 7. Values of I_c with respect to thunderstorm occurrence for various predictors in combination with SK index. The abbreviation "WSPD" refers to wind speed, other abbreviations are as in the text. Predictors are derived from 1700 GMT VAS retrievals, 1600 GMT surface observations, and from radar climatology.

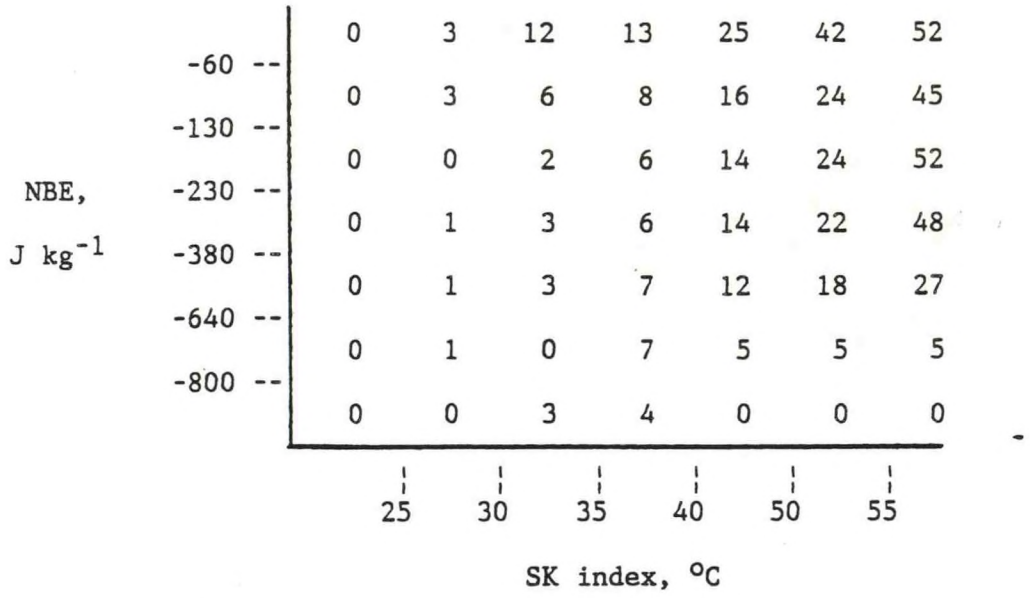

Figure 8. Observed thunderstorm relative frequency, percent, as a function of SK index and negative buoyant energy (NBE). Predictors derived from 1700 GMT VAS retrievals; observations are from the period 2000-0000 GMT.

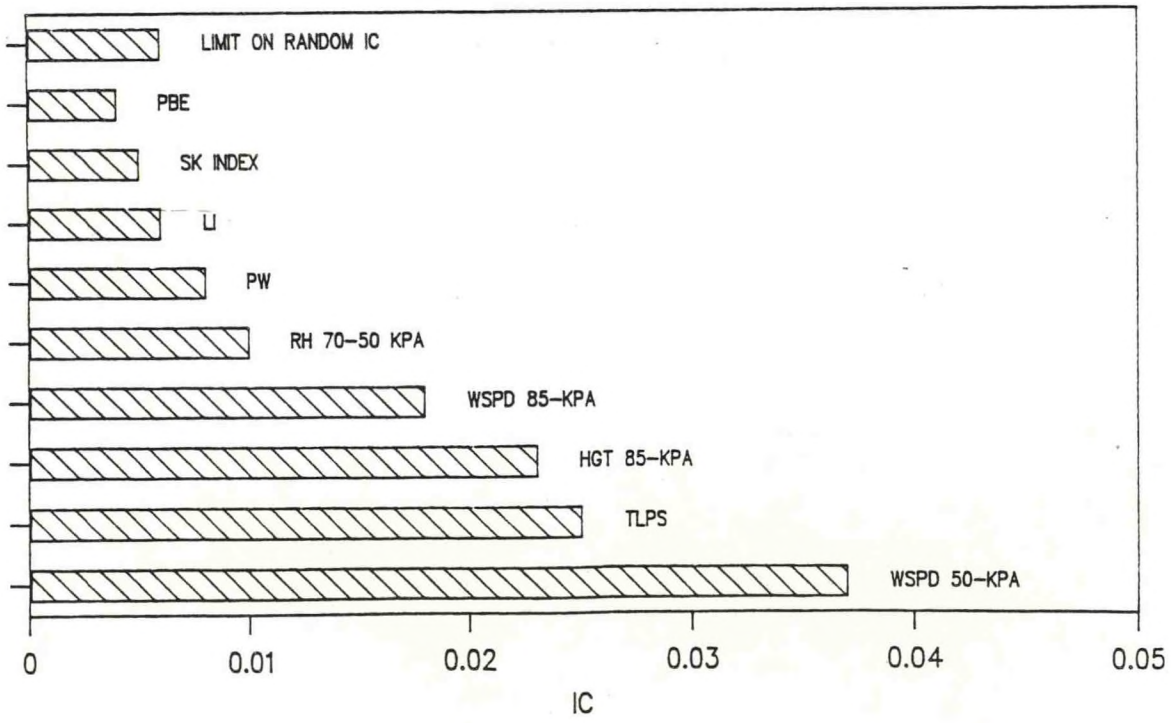

Figure 9. As in Fig. 1, except I_c is with respect to conditional severe local storm occurrence during the period 2000-0000 GMT. The abbreviation "HGT" refers to geopotential height, all other abbreviations are as in the text.

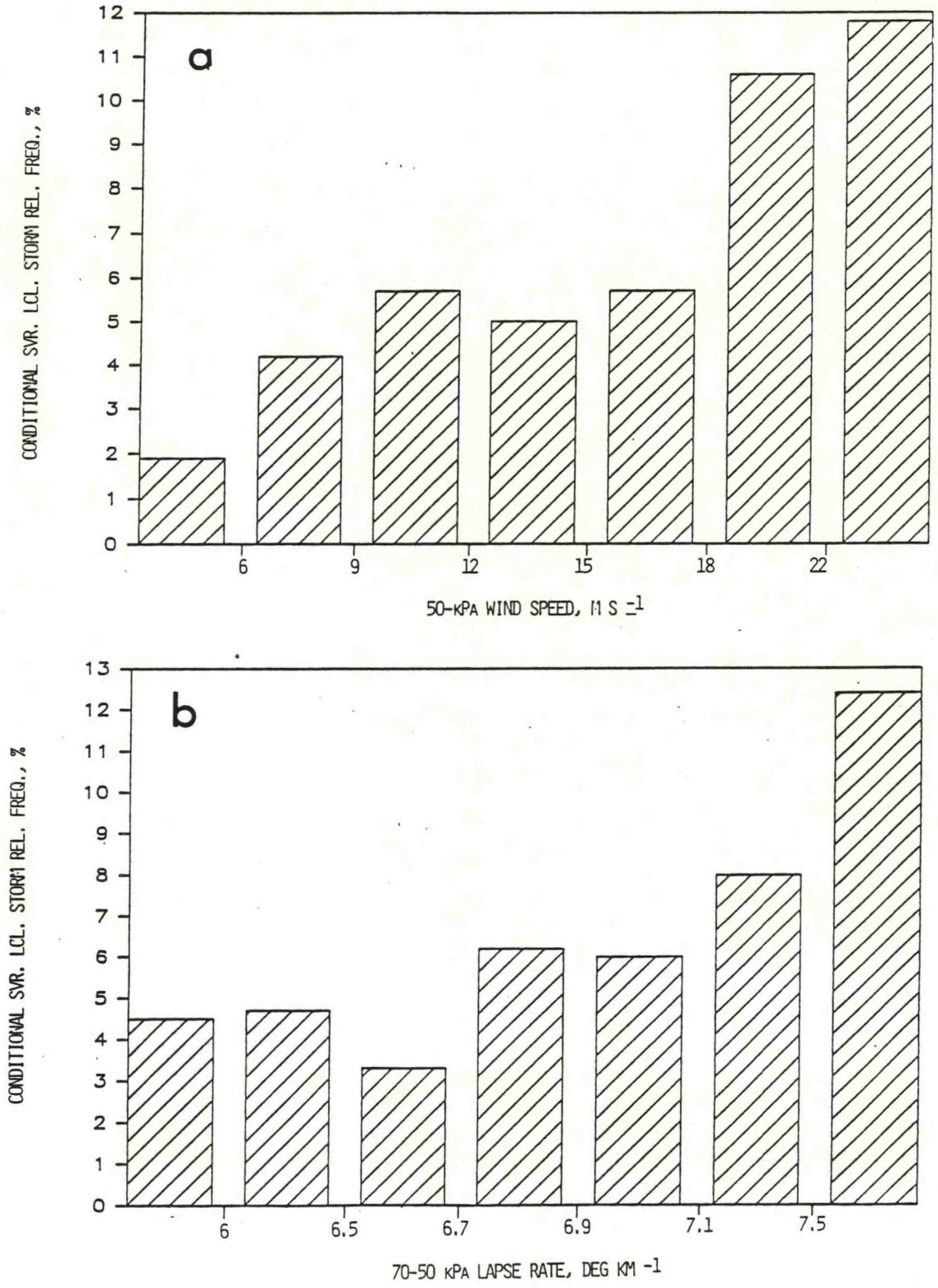

Figure 10. Observed severe local storm relative frequency within thunderstorm cases as a function of (a) 50-kPa wind speed, and (b) 70-50 kPa temperature lapse rate (TLPS). Storm events occurred during the period 2000-0000 GMT; predictors were derived from 1700 GMT VAS retrievals. Each category includes approximately 460 events.

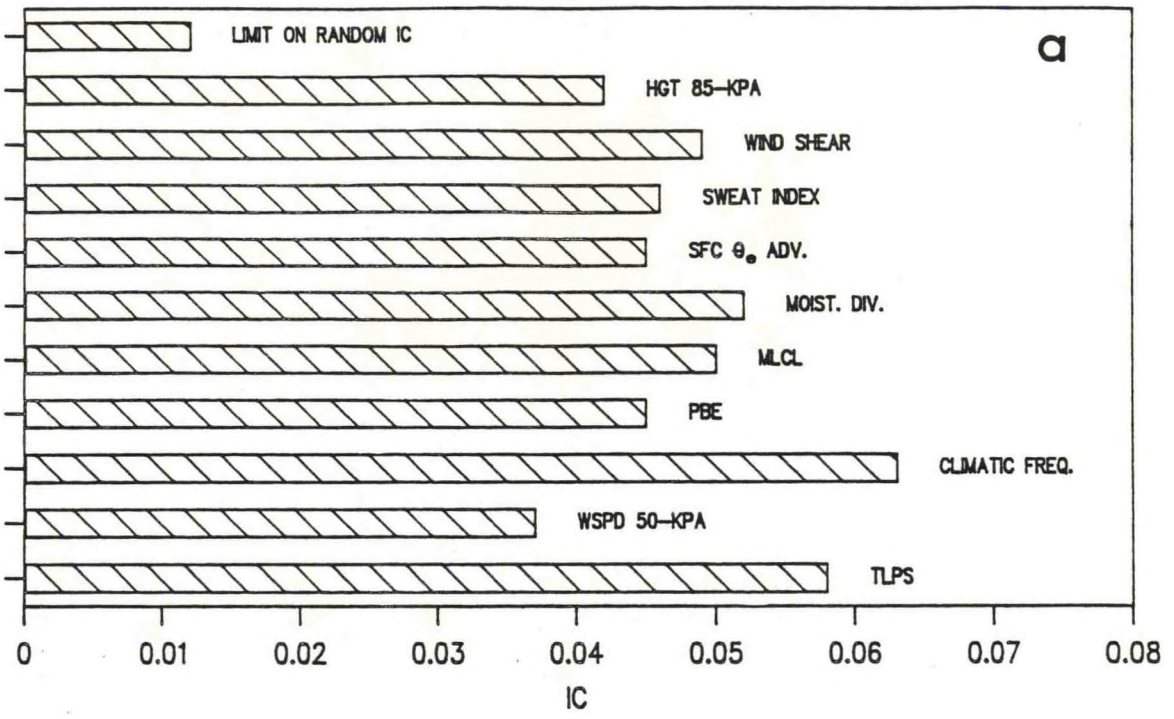

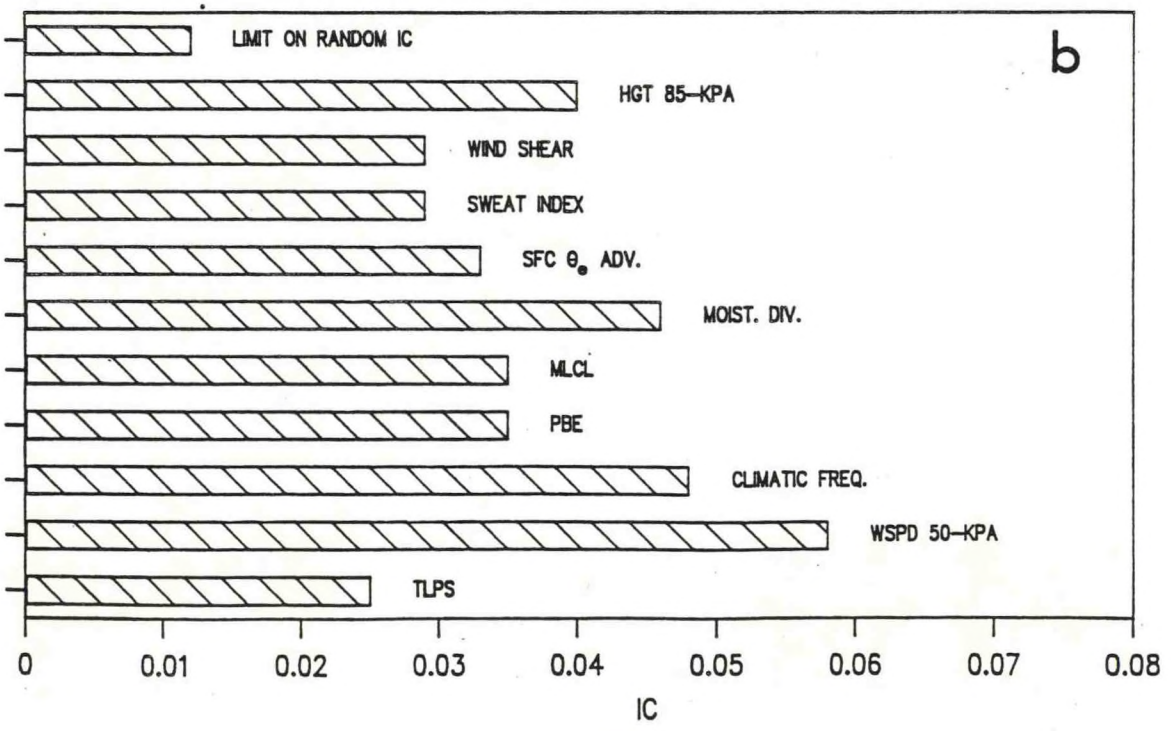

Figure 11. Values of I_c with respect to conditional severe local storm occurrence during the period 2000-0000 GMT, for various predictors in combination with (a) 50-kPa wind speed and (b) 70-50 kPa temperature lapse rate (TLPS).

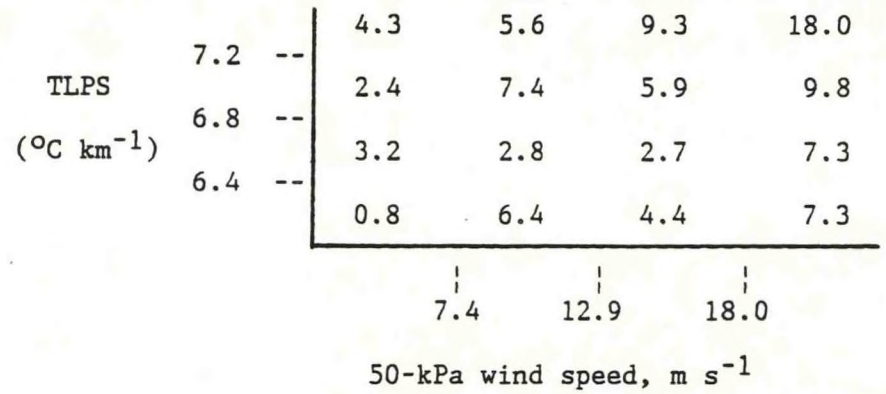

Figure 12. Conditional severe local storm relative frequency, percent, as a function of TLPS (vertical coordinate) and 50-kPa wind speed (horizontal coordinate). Predictors are derived from 1700 GMT VAS retrievals; observation period is 2000-0000 GMT.

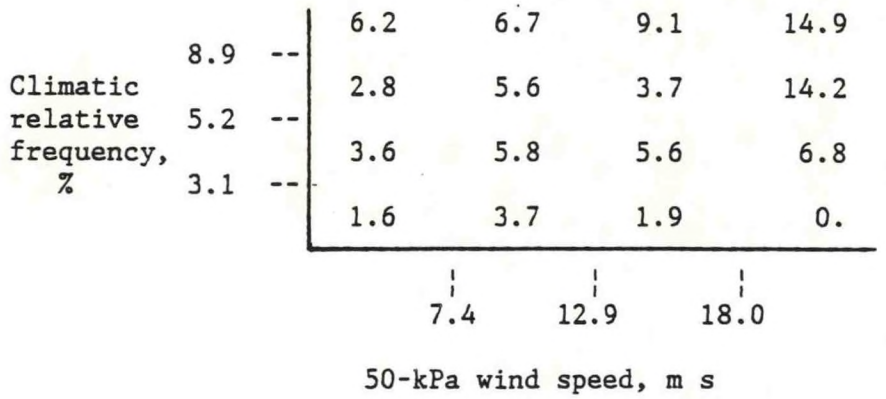

Figure 13. Conditional severe local storm relative frequency, per cent, as a function of climatic relative frequency (vertical coordinate) and 50-kPa wind speed (horizontal coordinate). Wind speed is derived from 1700 GMT VAS retrievals; climatic frequency based on 1974-1983 severe storm reports. Observation period is 2000-0000 GMT.

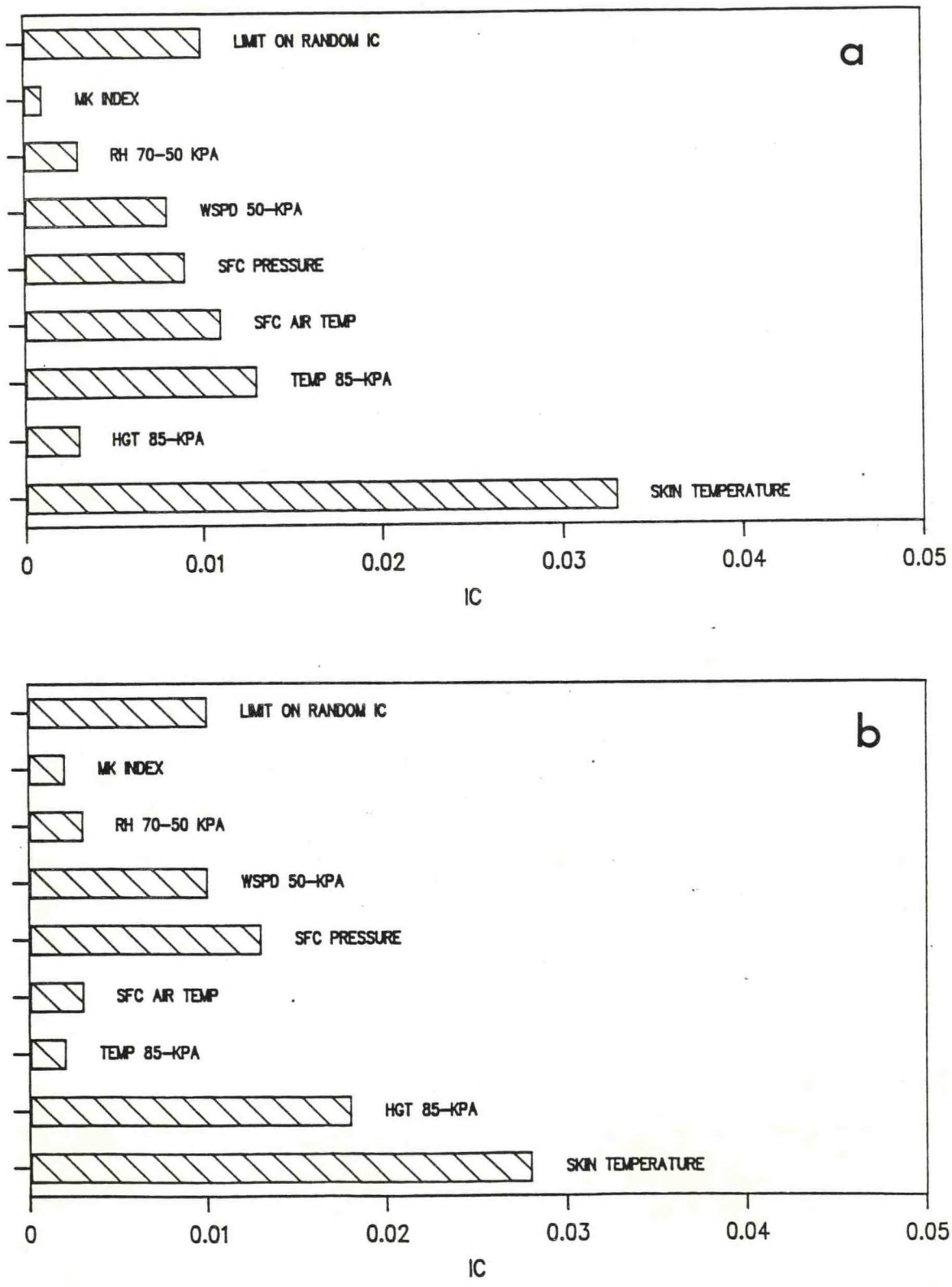

Figure 14. Values of I_c with respect to conditional severe local storm occurrence during the period 2000-0000 GMT, for (a) 3-h and (b) 6-h changes of various predictors. The 3-h changes are during the period 1400-1700 GMT; 6-h changes are during the period 1100-1700 GMT.

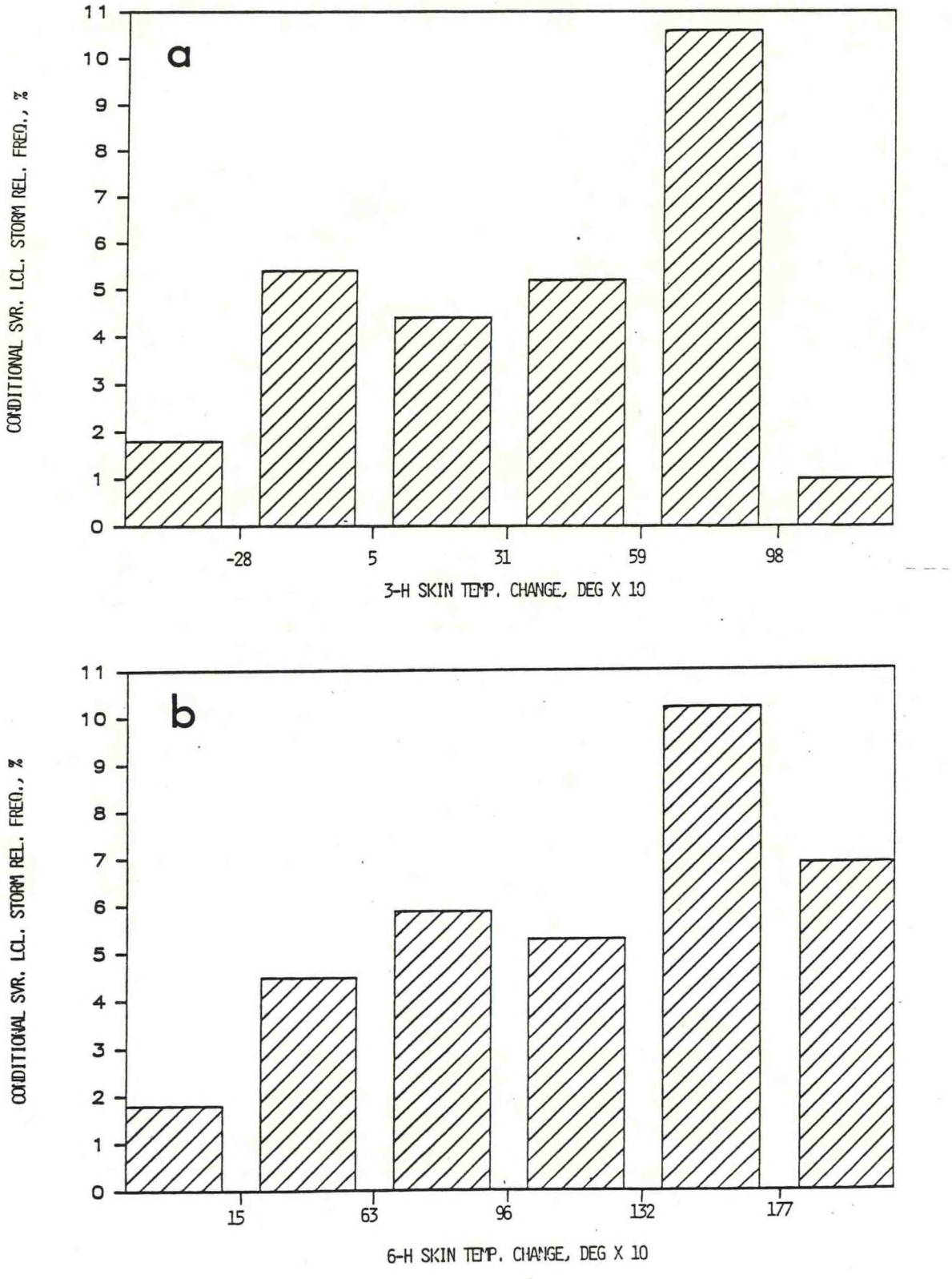

Figure 15. As in Fig. 7, except predictors are (a) 3-h and (b) 6-h change in skin temperature prior to 1700 GMT. Each category includes approximately 360 cases.

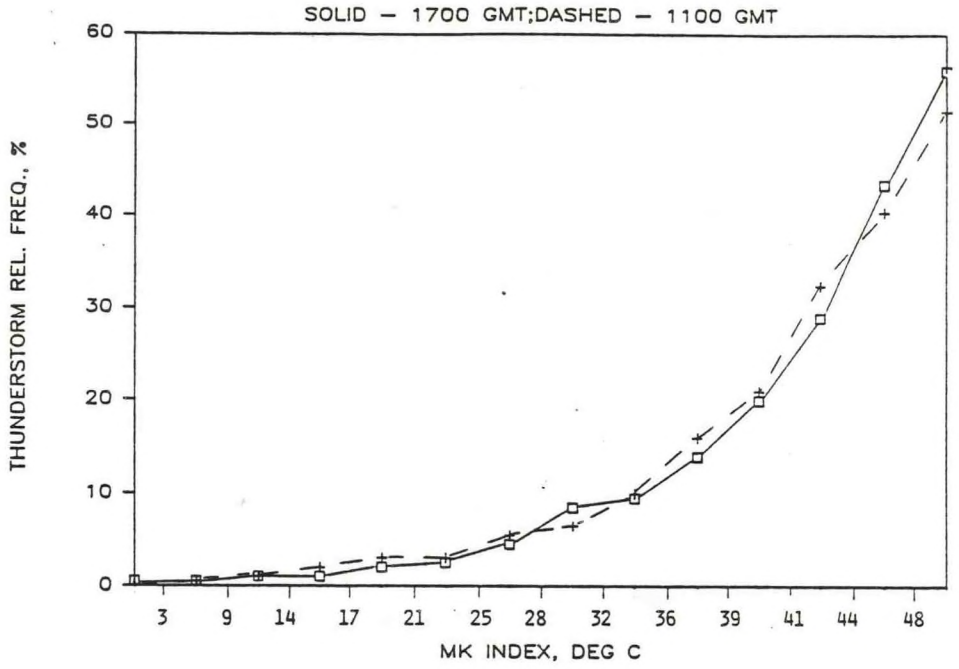

Figure 16. Observed thunderstorm relative frequency as a function of MK index derived from VAS retrievals at 1700 GMT (solid line) and at 1100 GMT (dashed line). Class interval dividers are for the MK index distribution at 1700 GMT.

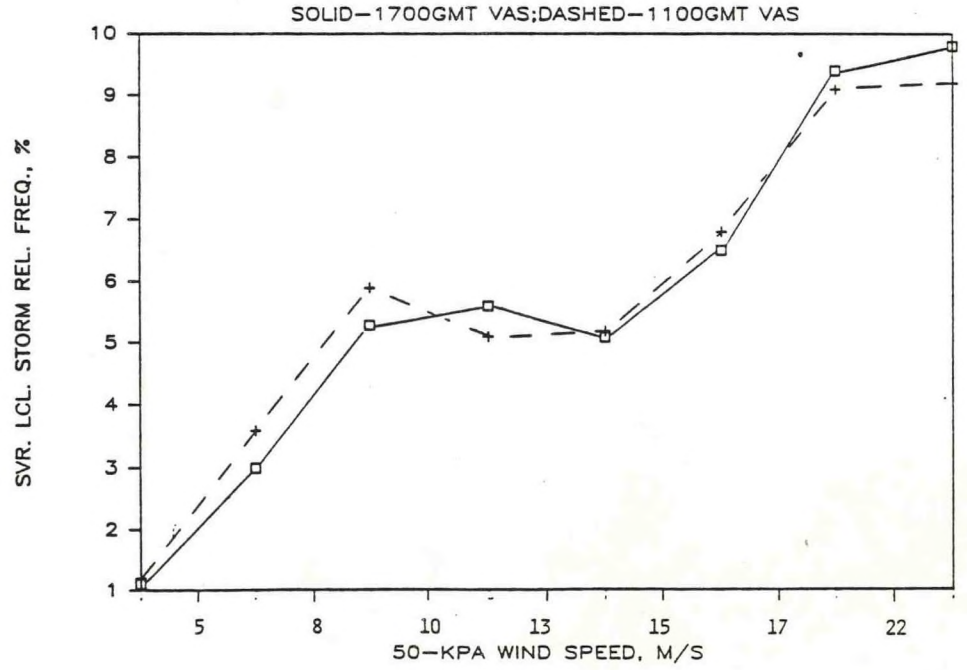

Figure 17. As in Fig. 16, except conditional severe local storm relative frequency as a function of 50-kPa wind speed. Class interval dividers are for the wind speed distribution at 1700 GMT.

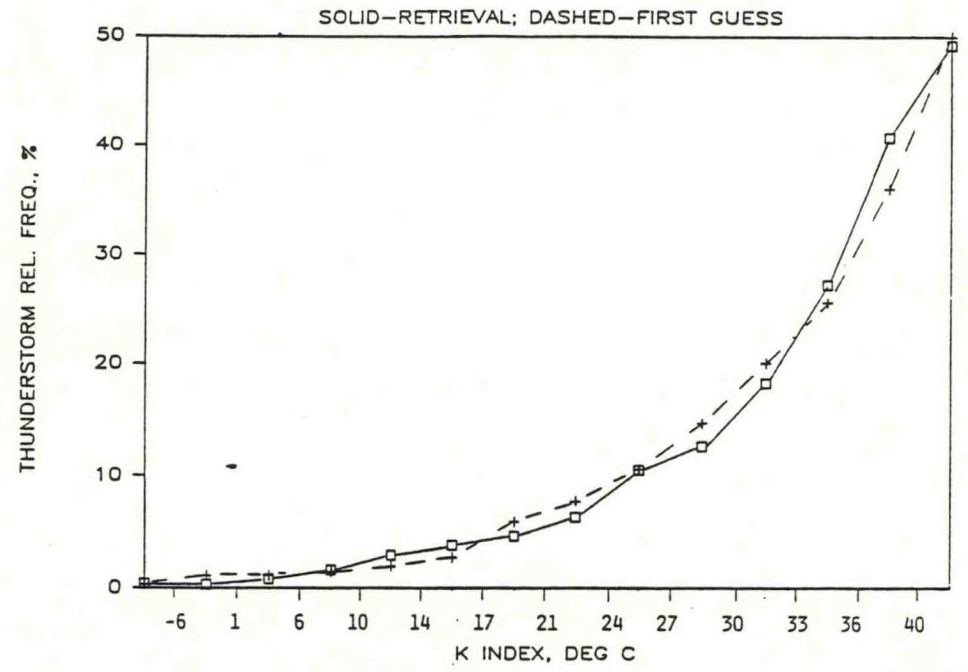

Figure 18. Observed thunderstorm relative frequency during the period 2000-0000 GMT as a function of K index derived from VAS retrievals at 1700 GMT (solid line) and from the retrieval first guess (dashed line). Class interval dividers are for the retrieval K index distribution.

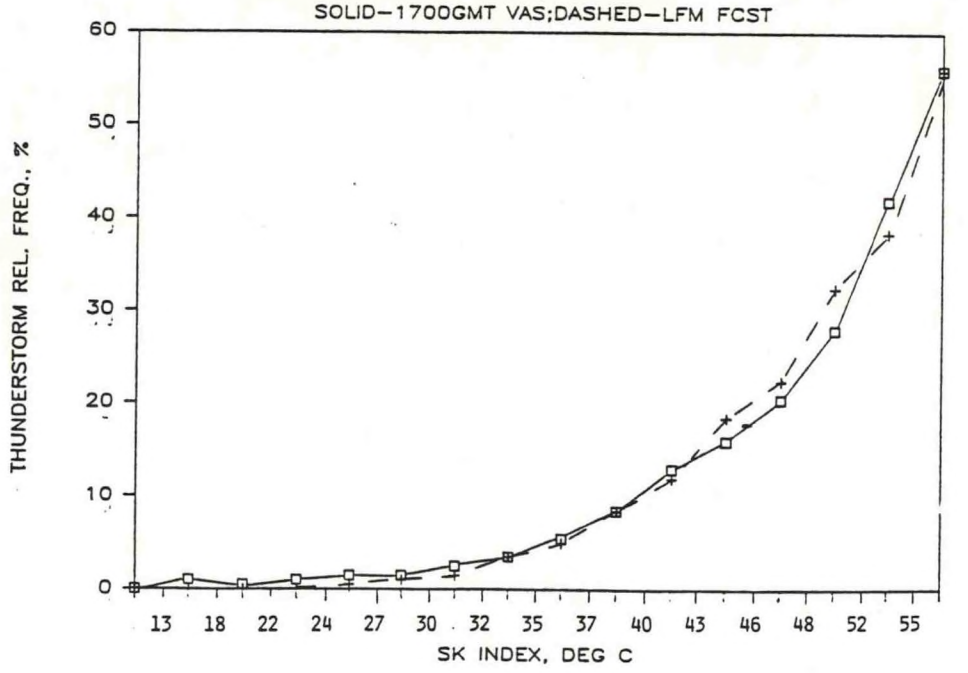

Figure 19. Observed thunderstorm relative frequency as a function of SK index derived from VAS retrievals at 1700 GMT (solid line) and from 12-h LFM forecasts valid at 0000 GMT (dashed line). Class interval dividers are for the VAS-derived SK index distribution.

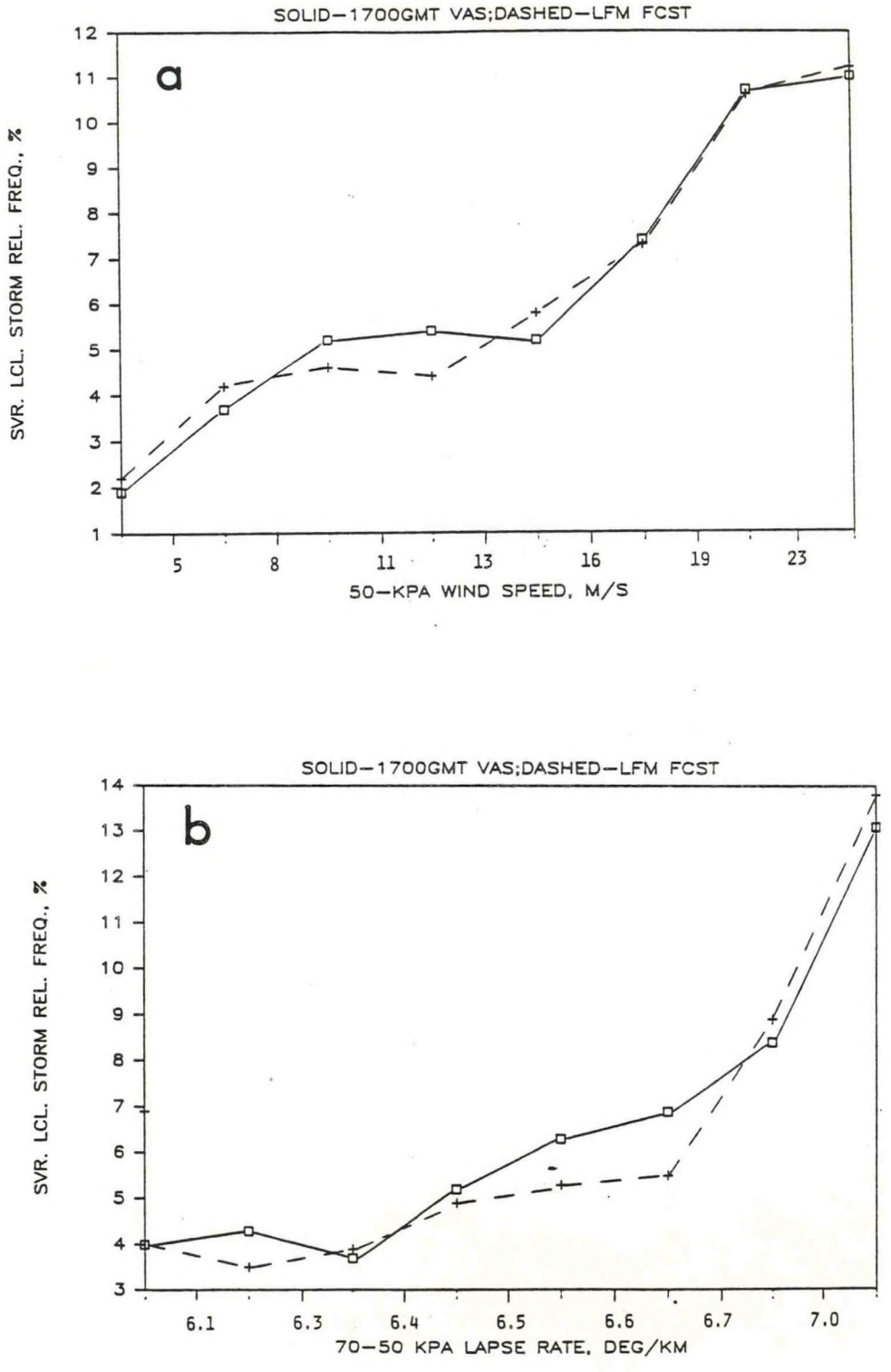

Figure 20. As in Fig. 19, except conditional severe local storm relative frequency as a function of (a) 50-kPa wind speed and (b) 70-50 kPa temperature lapse rate. In both (a) and (b), the class interval dividers are for the VAS-derived quantity.

(Continued from inside front cover)

NOAA Technical Memorandums

NWS TDL 43 Air-Sea Energy Exchange in Lagrangian Temperature and Dew Point Forecasts. Ronald M. Reap, October 1971, 23 pp. (COM-71-01112)

NWS TDL 44 Use of Surface Observations in Boundary-Layer Analysis. H. Michael Mogil and William D. Bonner, March 1972, 16 pp. (COM-72-10641)

NWS TDL 45 The Use of Model Output Statistics (MOS) To Estimate Daily Maximum Temperatures. John R. Annett, Harry R. Glahn, and Dale A. Lowry, March 1972, 14 pp. (COM-72-10753)

NWS TDL 46 SPLASH (Special Program to List Amplitudes of Surges From Hurricanes): I. Landfall Storms. Chester P. Jelesnianski, April 1972, 52 pp. (COM-72-10807)

NWS TDL 47 Mean Diurnal and Monthly Height Changes in the Troposphere Over North America and Vicinity. August F. Korte and DeVer Colson, August 1972, 30 pp. (COM-72-11132)

NWS TDL 48 Synoptic Climatological Studies of Precipitation in the Plateau States From 850-, 700-, and 500-Millibar Lows During Spring. August F. Korte, Donald L. Jorgensen, and William H. Klein, August 1972, 130 pp. (COM-73-10069)

NWS TDL 49 Synoptic Climatological Studies of Precipitation in the Plateau States From 850-Millibar Lows During Fall. August F. Korte and DeVer Colson, August 1972, 56 pp. (COM-74-10464)

NWS TDL 50 Forecasting Extratropical Storm Surges for the Northeast Coast of the United States. N. Arthur Pore, William S. Richardson, and Herman P. Perrotti, January 1974, 70 pp. (COM-74-10719)

NWS TDL 51 Predicting the Conditional Probability of Frozen Precipitation. Harry R. Glahn and Joseph R. Bocchieri, March 1974, 33 pp. (COM-74-10909)

NWS TDL 52 SPLASH (Special Program to List Amplitudes of Surges From Hurricanes): Part Two. General Track and Variant Storm Conditions. Chester P. Jelesnianski, March 1974, 55 pp. (COM-74-10925)

NWS TDL 53 A Comparison Between the Single Station and Generalized Operator Techniques for Automated Prediction of Precipitation Probability. Joseph R. Bocchieri, September 1974, 20 pp. (COM-74-11763)

NWS TDL 54 Climatology of Lake Erie Storm Surges at Buffalo and Toledo. N. Arthur Pore, Herman P. Perrotti, and William S. Richardson, March 1975, 27 pp. (COM-75-10587)

NWS TDL 55 Dissipation, Dispersion and Difference Schemes. Paul E. Long, Jr., May 1975, 33 pp. (COM-75-10972)

NWS TDL 56 Some Physical and Numerical Aspects of Boundary Layer Modeling. Paul E. Long, Jr. and Wilson A. Shaffer, May 1975, 37 pp. (COM-75-10980)

NWS TDL 57 A Predictive Boundary Layer Model. Wilson A. Shaffer and Paul E. Long, Jr., May 1975, 44 pp. (PB-265-412)

NWS TDL 58 A Preliminary View of Storm Surges Before and after Storm Modifications for Alongshore-Moving Storms. Chester P. Jelesnianski and Celso S. Barrientos, October 1975, 16 pp. (PB-247-362)

NWS TDL 59 Assimilation of Surface, Upper Air, and Grid-Point Data in the Objective Analysis Procedure for a Three-Dimensional Trajectory Model. Ronald M. Reap, February 1976, 17 pp. (PB-256-082)

NWS TDL 60 Verification of Severe Local Storms Warnings Based on Radar Echo Characteristics. Donald S. Foster, June 1976, 9 pp. plus supplement. (PB-262-417)

NWS TDL 61 A Sheared Coordinate System for Storm Surge Equations of Motion With a Mildly Curved Coast. Chester P. Jelesnianski, July 1976, 52 pp. (PB-261-956)

NWS TDL 62 Automated Prediction of Thunderstorms and Severe Local Storms. Ronald M. Reap and Donald S. Foster, April 1977, 20 pp. (PB-268-035)

NWS TDL 63 Automated Great Lakes Wave Forecasts. N. Arthur Pore, February 1977, 13 pp. (PB-265-854)

NWS TDL 64 Operational System for Predicting Thunderstorms Two to Six Hours in Advance. Jerome P. Charba, March 1977, 24 pp. (PB-266-969)

NWS TDL 65 Operational System for Predicting Severe Local Storms Two to Six Hours in Advance. Jerome P. Charba, May 1977, 36 pp. (PB-271-147)

NWS TDL 66 The State of the Techniques Development Laboratory's Boundary Layer Model: May 24, 1977. P. E. Long, W. A. Shaffer, J. E. Kemper, and F. J. Hicks, April 1978, 58 pp. (PB-287-821)

NWS TDL 67 Computer Worded Public Weather Forecasts. Harry R. Glahn, November 1978, 25 pp. (PB-291-517)

NWS TDL 68 A Simple Soil Heat Flux Calculation for Numerical Models. Wilson A. Shaffer, May 1979, 16 pp. (PB-297-350)

NWS TDL 69 Comparison and Verification of Dynamical and Statistical Lake Erie Storm Surge Forecasts. William S. Richardson and David J. Schwab, November 1979, 20 pp. (PB80 137797)

NWS TDL 70 The Sea Level Pressure Prediction Model of the Local AFOS MOS Program. David A. Unger, April 1982, 33 pp. (PB82 215492)

NWS TDL 71 A Tide Climatology for Boston, Massachusetts. William S. Richardson, N. Arthur Pore, and David M. Feit, November 1982, 67 pp. (PB83 144196)

NWS TDL 72 Experimental Wind Forecasts From the Local AFOS MOS Program. Harry R. Glahn, January 1984, 60 pp. (PB84-155514)

NWS TDL 73 Trends in Skill and Accuracy of National Weather Service POP Forecasts. Harry R. Glahn, July 1984, 34 pp. (PB84 229053)

NWS TDL 74 Great Lakes Nearshore Wind Predictions from Great Lakes MOS Wind Guidance. Lawrence D. Burroughs, July 1984, 21 pp. (PB85 212876/AS)

NWS TDL 75 Objective Map Analysis for the Local AFOS MOS Program. Harry R. Glahn, Timothy L. Chambers, William S. Richardson, and Herman P. Perrotti, March 1985, 35 pp. (PB85 212884/AS)

NWS TDL 76 The Application of Cumulus Models to MOS Forecasts of Convective Weather. David H. Kitzmiller, June 1985, 50 pp. (PB86 136686)

NWS TDL 77 The Moisture Model for the Local AFOS MOS Program. David A. Unger, December 1985, 41 pp. (PB86 151305)

DEPARTMENT OF COMMERCE · UNITED STATES · 75

Stimulating America's Progress
1913-1988